PB-222 237

RELATIONSHIP BETWEEN FABRIC STRUCTURE AND FILTRATION PERFORMANCE IN DUST FILTRATION

NATIONAL ENVIRONMENTAL RESEARCH CENTER

JULY 1973

Distributed By:

NTIS

National Technical Information Service
U. S. DEPARTMENT OF COMMERCE

PB 222 237

EPA-R2-73-288
July 1973

RELATIONSHIP BETWEEN FABRIC STRUCTURE AND FILTRATION PERFORMANCE IN DUST FILTRATION

Reproduced by
NATIONAL TECHNICAL
INFORMATION SERVICE
U S Department of Commerce
Springfield VA 22151

77

Office of Research and Monitoring
National Environmental Research Center
U.S. Environmental Protection Agency
Research Triangle Park, N.C. 27711

EPA-R2-73-288

RELATIONSHIP BETWEEN FABRIC STRUCTURE AND FILTRATION PERFORMANCE IN DUST FILTRATION

by

Dean C. Draemel

Control Systems Laboratory
National Environmental Research Center
Research Triangle Park, North Carolina 27711

Project 21ADJ51
Program Element 1A2012

NATIONAL ENVIRONMENTAL RESEARCH CENTER
OFFICE OF RESEARCH AND MONITORING
U.S. ENVIRONMENTAL PROTECTION AGENCY
RESEARCH TRIANGLE PARK, NORTH CAROLINA 27711

July 1973

RESEARCH REPORTING SERIES

Research reports of the Office of Research and Monitoring, Environmental Protection Agency, have been grouped into five series. These five broad categories were established to facilitate further development and application of environmental technology. Elimination of traditional grouping was consciously planned to foster technology transfer and a maximum interface in related fields. The five series are:

1. Environmental Health Effects Research
2. Environmental Protection Technology
3. Ecological Research
4. Environmental Monitoring
5. Socioeconomic Environmental Studies

This report has been assigned to the Environmental Protection Technology Series. This series describes research performed to develop and demonstrate instrumentation, equipment and methodology to repair or prevent environmental degradation from point and non-point sources of pollution. This work provides the new or improved technology required for the control and treatment of pollution sources to meet environmental quality standards.

EPA REVIEW NOTICE

This report has been reviewed by the Office of Research and Monitoring, EPA, and approved for publication. Approval does not signify that the contents necessarily reflect the views and policies of the Environmental Protection Agency, nor does mention of trade names or commercial products constitute endorsement or recommendation for use.

BIBLIOGRAPHIC DATA SHEET	1. Report No. EPA-R2-73-288	2.	3. Recipient's Accession No. PB-222 237
4. Title and Subtitle Relationship Between Fabric Structure and Filtration Performance in Dust Filtration			5. Report Date July 1973 6.
7. Author(s) Dean C. Draemel			8. Performing Organization Rept. No.
9. Performing Organization Name and Address EPA, Office of Research and Development NERC-RTP, Control Systems Laboratory Research Triangle Park, North Carolina 27711			10. Project/Task/Work Unit No. 21 ADJ 51 11. Contract/Grant No. In-house Report
12. Sponsoring Organization Name and Address			13. Type of Report & Period Covered Final 14.

15. Supplementary Notes

16. Abstracts The report identifies a semi-empirical relationship between clean cloth fabric structural parameters, dust parameters, and filtration performance. High outlet concentration caused by bleeding or seepage of dust is a function of the pore size distribution of the fabric vs. size properties of the dust. A significant number of pores with a characteristic dimension roughly 10 times the mass mean particle diameter of the dust being filtered leads to bleeding and seepage of dust. This conclusion results from studies with three dusts (fly ash, limestone, and silica), a number of fiber types, and a range of fabric construction variables. Pressure-related filtration performance can be correlated with clean fabric free area if yarn boundaries are well defined. Since many yarn boundaries are not well defined, clean cloth Frazier permeability may be used as an alternative method of correlating pressure-related filtration performance.

17. Key Words and Document Analysis. 17a. Descriptors

Air Pollution
Fabrics
Dust
Filtration
Fly Ash
Limestone
Silicon Dioxide
Fibers
Yarns
Interstices
Woven Fabric
Seepage

17b. Identifiers/Open-Ended Terms

Air Pollution Control
Stationary Sources
Yarn Boundaries
Frazier Permeability
Baghouse

17c. COSATI Field/Group 13B, 7A, 11E, 13H, 14B

18. Availability Statement: Unlimited

19. Security Class (This Report) UNCLASSIFIED — 21. No. of Pages 77

20. Security Class (This Page) UNCLASSIFIED — 22. Price $3.75 / 1.45

NTIS-35 (REV. 3-72)
USCOMM-DC 14952-P72

ABSTRACT

The report identifies a semi-empirical relationship between clean cloth-fabric structural parameters, dust parameters, and filtration performance. The criterion for high outlet concentration as a result of bleeding or seepage of dust is a function of the pore size distribution of the fabric versus size properties of the dust. The presence of a significant number of pores with a characteristic dimension roughly 10 times the mass mean particle diameter of the dust being filtered leads to bleeding and seepage of dust. This conclusion results from studies with three dusts (fly ash, limestone, and silica), a number of fiber types, and a range of fabric construction variables. Pressure-related filtration performance can be correlated against clean fabric free area if well defined yarn boundaries are present. Since filtration fabric yarn boundaries are generally not well defined, pressure-related filtration performance can be correlated against clean cloth Frazier permeability.

CONTENTS

	Page
CONCLUSIONS	1
RECOMMENDATIONS	5
INTRODUCTION	7
Background	7
Reasons for Performing Work	7
Approach and Objectives	8
EQUIPMENT AND PROCEDURES	9
Single-Compartment Baghouses--Initial Study	9
Bench-Scale Filtration Apparatus--Supplemental Study	14
Single-Compartment Baghouses--Supplemental Study	14
RESULTS AND DISCUSSION	17
Single-Compartment Baghouse Study--Free-Area Correlation with Pressure-Related Filtration Response	17
Group 1 Fabrics	18
Group 2 Fabrics	23
Group 3 Fabrics	23
Group 4 Fabrics	30
Bench-Scale Filtration Study--Microscopic Analysis of the Filtration Process	34
Fabric 015	34
Fabric 038	37
Fabric 088	37
Fabric 120	38
Fabric 088 ($\bar{d}$=10μm Test Dust)	39

Preceding page blank

	Page
Single-Compartment Baghouse Study--Dust-Size/Pore-Size Correlation with Filter Efficiency	41
Filtration Performance of Dust/Fabric Combinations	41
Filtration Performance of Commercial Fabrics	45
Fabric Parameters Generating Significant Dust/Fabric Interactions	50
REFERENCES	55
NOMENCLATURE	57
CONVERSION FACTORS TO METRIC UNITS	59
APPENDIX A--DESCRIPTION OF 123 TEST FABRICS	61
I. Multifilament-Dacron Series	61
II. Staple-Dacron Series	63
APPENDIX B--STANDARD FABRIC AND YARN CHARACTERIZATION TESTS	65
I. Fabric Analysis	65
II. Yarn Analysis	67
APPENDIX C--EFFECT OF WEAVE ON FILTRATION PERFORMANCE	69
APPENDIX D--YARN AND FABRIC ANALYSIS	73
I. Fabric Analysis--Test Results	73
II. Yarn Analysis--Test Results (Denier, Bulk and Fiber Density)	74
III. Yarn Analysis--Test Results (Twist, Width, and Thickness)	75
APPENDIX E--RESULTS OF SUPPLEMENTAL CHARACTERIZATION TESTS AND FABRIC FILTRATION PERFORMANCE DATA*	

*Not included in this report, but available on request from author.

FIGURES

Figure No.	Title	Page
1	Single-Compartment Baghouse Test Equipment	10
2	Characteristic Resistance Curve	12
3	Bench-Scale Filtration Apparatus	15
4	ΔP_f and S_e Versus Free Area -- Group 1 Fabrics	20
5	K Versus Free Area -- Group 1 Fabrics	21
6	C_o Versus Free Area -- Group 1 Fabrics	22
7	ΔP_f and S_e Versus Free Area -- Group 2 Fabrics	25
8	K Versus Free Area -- Group 2 Fabrics	26
9	ΔP_f and S_e Versus Free Area -- Group 3 Fabrics	28
10	K Versus Free Area -- Group 3 Fabrics	29
11	ΔP_f and S_e Versus Free Area -- Group 4 Fabrics	32
12	K Versus Free Area -- Group 4 Fabrics	33
13	The Four Interstice Types	36
14	Pore Dimensions	48
15	Non-linear ΔP Versus t Response	51
16	Schematic Representation of Dust/Fabric Interactions	53

TABLES

Table No.	Title	Page
1	Free Area and Performance Data--Group 1 Fabrics (Dacron)	19
2	Free Area and Performance Data--Group 2 Fabrics	24
3	Free Area and Performance Data--Group 3 Fabrics	27
4	Free Area and Performance Data--Group 4 Fabrics	31
5	Fabric Description Data for Microscopic Analysis and Dust/Fabric Combination Studies	35
6	Minimum Pinhole Sizes During a Filter Cycle	40
7	Filtration Performance Data for Dust/Fabric Combinations	42
8	Relative Yarn Dimensions for Continuous-Filament Versus Staple Yarns Compared to Outlet Concentration Data	44
9	Filtration Performance Data--Fabric Composition Study	46
10	Pore Size Distributions of Selected Fabrics	49
C1	Pore Type Effects on Fabric Behavior	69
C2	Continuous-Filament Fabrics--Pore Type Effects	71
C3	Staple Yarn Fabrics--Pore Type Effects	72
C4	Minutes of Filtration to Form Continuous Dust Cake	72

CONCLUSIONS

Fabric filtration performance is dependent on structural properties of the fabric. Within the limits of this study (mainly fly ash at a standard set of test conditions) the following conclusions can be made:

1. Efficiency or outlet concentration is a function of the pore size distribution of a given fabric. Bleeding or leaking of dust is a function of the number of pores above a critical size which is related to size properties of the dust being filtered. This study indicates that the presence of a significant number of pores with a characteristic dimension roughly 10 times the characteristic dimension (a mass mean particle diameter) of the dust being filtered (fly ash, limestone, amorphous silica) leads to bleeding or leaking of dust; i.e., increased penetration. Projecting fibers within the pores and above the fabric's surface greatly reduce the effective characteristic pore dimension with respect to dust bridging. Such fibers do not significantly affect the gas flow through the pore; i.e., although efficiency is a function of projecting fibers, pressure drop is relatively unaffected. Although staple yarns provide less yarn cover per unit weight of fiber, as opposed to continuous filament yarns, the added benefit of the projecting fibers from staple yarns can be valuable.

2. K values (specific cake resistance) with a given dust are dependent on the structure of the underlying fabric. The deep channel-like pores, formed by more rounded yarns, can lead to significant deposition of dust under velocity conditions of an order of magnitude or more greater than the average face velocity of the fabric. Deposition at local increased velocity would tend to increase dust packing density and thus increase K.

(Dusts subject to cake collapse phenomena imply pressure and/or velocity dependence on dust packing density.) Very shallow pores and a smooth fabric surface with no projecting fibers can be very efficient in particle retention but lead to a completely unsupported dust layer which has a characteristically high K value and is subject to cake collapse as pressure increases. Projecting fibers appear to support a more porous dust cake (lower K values), less subject to cake collapse. The dense projecting fibers found with napped fabrics may tend to produce non-linear ΔP vs t response, indicating a deviation from the cake law type of filtration behavior normally seen with a woven fabric. K values with a given dust may vary considerably as a function of fabric even though efficiency remains relatively constant for the same dust/fabric combinations.

3. Effective drag (flow resistance of the cleaned filter fabric) can be correlated with free area if yarn boundaries are well defined. If yarn boundaries are not well defined, clean cloth permeability generally is a good indicator of effective filter drag. Factors such as deep, channel-like pores with no projecting fibers appear to increase effective filter drag values for the aged filter fabrics just as the K values are increased.

4. Structural properties of a fabric strongly affect the filtration performance of a fabric and the fabric's interaction with a dust. The chemical composition of the fiber does not appear to be a major variable although intrinsic properties of certain fiber types, such as the curly nature of cotton, may modify or determine significant structural features of a fabric.

5. Fabric parameters such as weave and yarn construction also interact to influence significant structural properties of a fabric; i.e., pore depth which in turn affects performance.

RECOMMENDATIONS

1. Bench-scale filtration tests and microscopic examination of potential filters with the dust and system (temperature, relative humidity, etc.) of interest will provide design data and insight into the probable performance. This will allow determination of significant dust fabric interactions such as bleeding criteria and relative K values of dust fabric combinations for the application under consideration. Care must be taken to perform such tests with the dust and conditions expected in the application because performance may be affected by dust properties and system variables such as relative humidity.

2. Additional work should be conducted to extend the limits of this work to a greater range of operating conditions and more dust/fabric combinations.

3. An attempt should be made to more exactly define the criteria for bridging and bleeding as a function of dust and pore properties.

4. Performance of operating fabric filter systems should be observed in the field to provide practical data useful in future design and specifications of fabrics for industrial dust and fume control.

Preceding page blank

INTRODUCTION

BACKGROUND

Much literature exists concerning flow and pressure drop through porous media. Refinements and simplifying assumptions must be made when considering dust filtration through porous media. When considering dust filtration through heterogeneous (woven fabrics) versus homogeneous porous media (mats, felts, papers, membranes, etc.), the situation becomes increasingly complex.

Exact theoretical treatment of dust filtration through woven fabrics is largely impossible without geometrical simplifications. Actual industrial fabric filters seldom correspond to screens, monofilament fabrics, arrays of perfect orifices, or single fibers as assumed in theoretical analyses.

General empirical correlations can be developed but, lacking any fundamental backup, are often subject to catastrophic failures occurring almost randomly. Improved relationships between fabric structure and filtration performance should result from practical considerations of theory and empiricism.

REASONS FOR PERFORMING WORK

Preliminary work relating fabric structure to filtration performance was conducted by Spaite and Walsh.[1] This work pointed out significant changes in performance with what appeared to be relatively small changes in fabric structure. Analysis of filtration literature by Borgwardt and Durham[2] cites the fact that equations normally used to predict filter-house pressure drops "assume dust drag to be determined by intrinsic properties of the dust only."

Preceding page blank

The Kozeny[3] equation, (1), relates pressure versus flow through porous media for a bed of fixed configuration:

$$\frac{\Delta P}{u_f} = J \frac{g_1}{g_c} \frac{\mu L}{C_K} \left(\frac{A_p}{V_p}\right)^2 \frac{(1-\alpha)^2}{\alpha^3} \qquad (1)$$

This equation can be used to describe pressure drop through a filter cake as a function of time if the dust feed rate and gas properties are held constant. Under these conditions, cake law filtration (linear ΔP vs t) results when L increases linearly with time and α is constant. If α is not constant, L will increase non-linearly with t generating a non-linear ΔP vs t filtration response. Implications of differing K (specific cake resistance proportional to $\frac{\Delta P}{\Delta t}$) values with the same dust on different fabrics and the occasional non-linear pressure response of some fabrics are that α is a function of the fabric; i.e., K is not solely an intrinsic property of a given dust alone.

Durham and Harrington[4] showed a significant interaction of fabrics and dusts as a function of relative humidity. Their research, along with a number of other smaller studies, has led to the development of the program reported here.

APPROACH AND OBJECTIVES

Slight variations in fabric structure have been shown to significantly affect filter performance. No quantitative determination has been made of exactly what factors are responsible for the observed changes in filtration performance. The objective of this study was to relate performance to clean cloth fabric parameters, and to obtain quantitative relationships with such parameters.

EQUIPMENT AND PROCEDURES

SINGLE-COMPARTMENT BAGHOUSES--INITIAL STUDY

A group of 123 fabrics (listed in Appendix A) was custom woven and sewn into filter bags. These fabrics were subjected to a number of standard fabric characterization tests (listed in Appendix B). Results of these standard tests were used to obtain an accurate quantitative description of the structure of each fabric. The filter bags of each fabric were tested on single-compartment, highly instrumented baghouses to characterize the fabric's filtration performance. Results of the supplemental characterization tests and the filtration performance data for each fabric are listed in Appendix E. (Appendix E is not included in this report. It is available on request.)

A single-compartment, instrumented baghouse is shown schematically in Figure 1.

Dust-laden air, entering at the top of the baghouse, is deposited on the inside of the bag. The air stream then passes out of the baghouse, through a venturi flow-measuring device, flow control valve, efficiency sampling section, and a positive-displacement rotary blower. The air stream is conditioned in a controlled-humidity controlled-temperature chamber before entering the flow system. Dust is fed by a variable speed screw feeder and a dispersion venturi. The baghouses are equipped with adjustable timers to automatically control filtration time, shake time, and delay time. Flow volume through the filter bags is automatically controlled and both flow and pressure drop through the bags are continuously recorded.

Test filters of each of the 123 fabrics were 5.56 in.* in diameter and 71.5 in. in overall length with a 2-in. cuff on each end. Total

*Although it is EPA's policy to use the metric system for quantitative descriptions, the British system is used in this report because not to do so would tend to confuse the reader. Readers who are more accustomed to metric units may use the table of conversions on Page 59 to facilitate the translation.

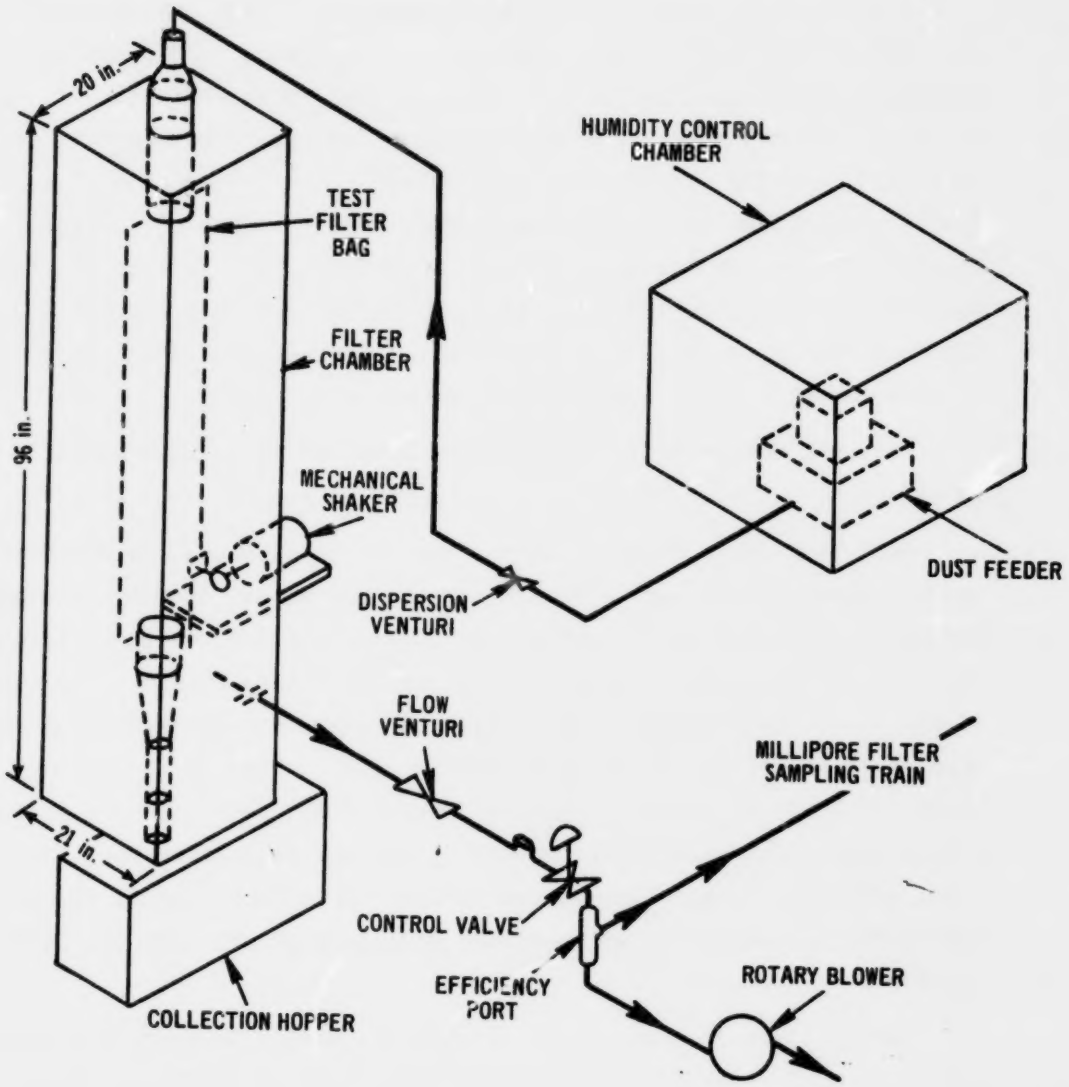

Figure 1. Single-compartment baghouse test equipment.

filter area was 8.1 ft^2. Flow was controlled at 32.5 acfm to provide a filter ratio of 4.0 ft/min. (4.0 fpm). Dust feed was set to give an inlet dust concentration of 3.0 grains/ft^3. The test dust was redispersed Detroit Edison fly ash which had been classified to remove coarse particles; i.e., > 20 μm. The test dust was 50 percent by weight less than 3.7 μm, and 90 percent by weight less than 11 μm by Coulter Counter analysis. Relative humidity of the gas stream was controlled at 30 ±5% at 70 ±10°F. Filter bags were installed with no apparent slack under a very slight tension (estimated at ~ 1 lb). Each filter bag was run for 24 hours at the conditions specified to break in the fabric and allow it to attain rough equilibrium. The filter cycle consisted of 20 minutes of filtration, a 1-minute delay, 2 minutes of shaking, and another 1-minute delay before repeating the cycle. The bottom of the bag was shaken with a horizontal shake 1-3/4 in. in length, at a frequency of 240 cycles per minute.

A sample of 4.0 acfm was withdrawn isokinetically through a probe downstream of the filter bag. The sample was drawn through a 0.45 μm Millipore filter. A Coulter Counter analysis was run on the dust sample collected. Efficiency was calculated by the weight of dust collected versus the known dust feed rate. Fallout was not measured but was assumed to be reasonably constant at an insignificant level for the fixed dust, bag dimensions, and flow conditions used. Each filter bag was sampled for three consecutive cycles after the 24-hour equilibration period. Filtration performance data recorded in Appendix E (available on request) represent the averages from the three consecutive cycles.

A typical pressure drop versus areal dust loading curve for a fabric filter is shown in Figure 2. Four responses describing fabric performance are taken from this curve and the Millipore filter dust sample. The linear portion of the curve, representing cake law filtration, is described by:

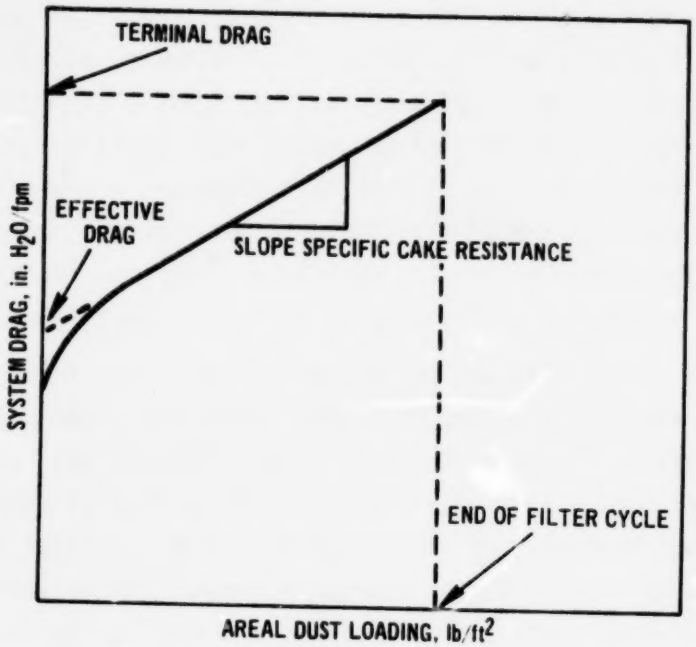

Figure 2. Characteristic resistance curve.

$$\frac{\Delta P \ A}{Q} = K\bar{w} + S_e \qquad (2)$$

The three responses describing system resistance are:

effective drag, $S_e \left(\frac{\text{in. } H_2O}{\text{ft/min}}\right)$

specific cake resistance, $K \left(\frac{\text{in. } H_2O/\text{ft/min}}{\text{lb/ft}^2}\right)$

terminal drag $\frac{\Delta P_f \ A}{Q} \left(\frac{\text{in. } H_2O}{\text{ft/min}}\right)$

where $\bar{w}$ is the areal dust loading in lb/ft^2. For the data reported in this paper, final pressure drop, ΔP_f (in. H_2O), is used in place of terminal drag. For a given filtration cycle, only two of the three responses are independent; however, performance is more easily visualized with the aid of the three responses. The fourth response, outlet concentration, represents an average over the filter cycle, and is calculated from the Millipore sample by using:

$$C_o = \frac{\text{weight on Millipore}}{\text{sample volume}} \qquad (3)$$

Inlet dust concentration is defined as:

$$C_i = \frac{R}{Q} \qquad (4)$$

The efficiency is thus:

$$\text{Eff} = 1 - \frac{C_o}{C_i} \quad \text{weight percent.} \qquad (5)$$

BENCH-SCALE FILTRATION APPARATUS--SUPPLEMENTAL STUDY

Selected fabrics from the 123 fabrics tested on the pilot-scale baghouses were also tested on a small bench-scale filter system. This bench-scale apparatus, shown in Figure 3, consists of a grooved-disc dust feeder, filter chamber, filter holder, blower, and rotameter. Pressure drop across the filter was measured by an inclined manometer.

Dust was fed to the lower face of the horizontally mounted filter. The 1-ft^2 filter fabric was held in a removable frame, clamped between the filter chamber sections. The fabric was tensioned slightly by hand, to hold it firm and flat in the frame. The frame consisted of two pieces of 1/4-in. plastic with a 1-ft^2 section cut out of the center. The fabric was placed between the frame sections and the assembly was bolted together. A thin strip of soft rubber provided an airtight gasket against both sides of the fabric and between the filter frame and the filter chamber sections.

Dust was fed and the pressure increase was recorded as a function of time. The flow was stopped and the filter fabric frame was removed occasionally to allow microscopic examination and weighing. Weighings, used to calculate dust/fabric resistance coefficients (K values), did not represent efficiency because of the relatively large amount of dust that settled in the filter chamber sections. Photomicrographs were taken of the dust/fabric surface at various times throughout the filter cycle. Since pertinent information from the limited number of runs on the bench-scale filtration apparatus was fairly qualitative in nature, it is not presented as a data summary in an appendix.

SINGLE-COMPARTMENT BAGHOUSES--SUPPLEMENTAL STUDY

Additional runs were conducted on 9 fabrics with structural properties differing from those of the previously tested 123 fabrics

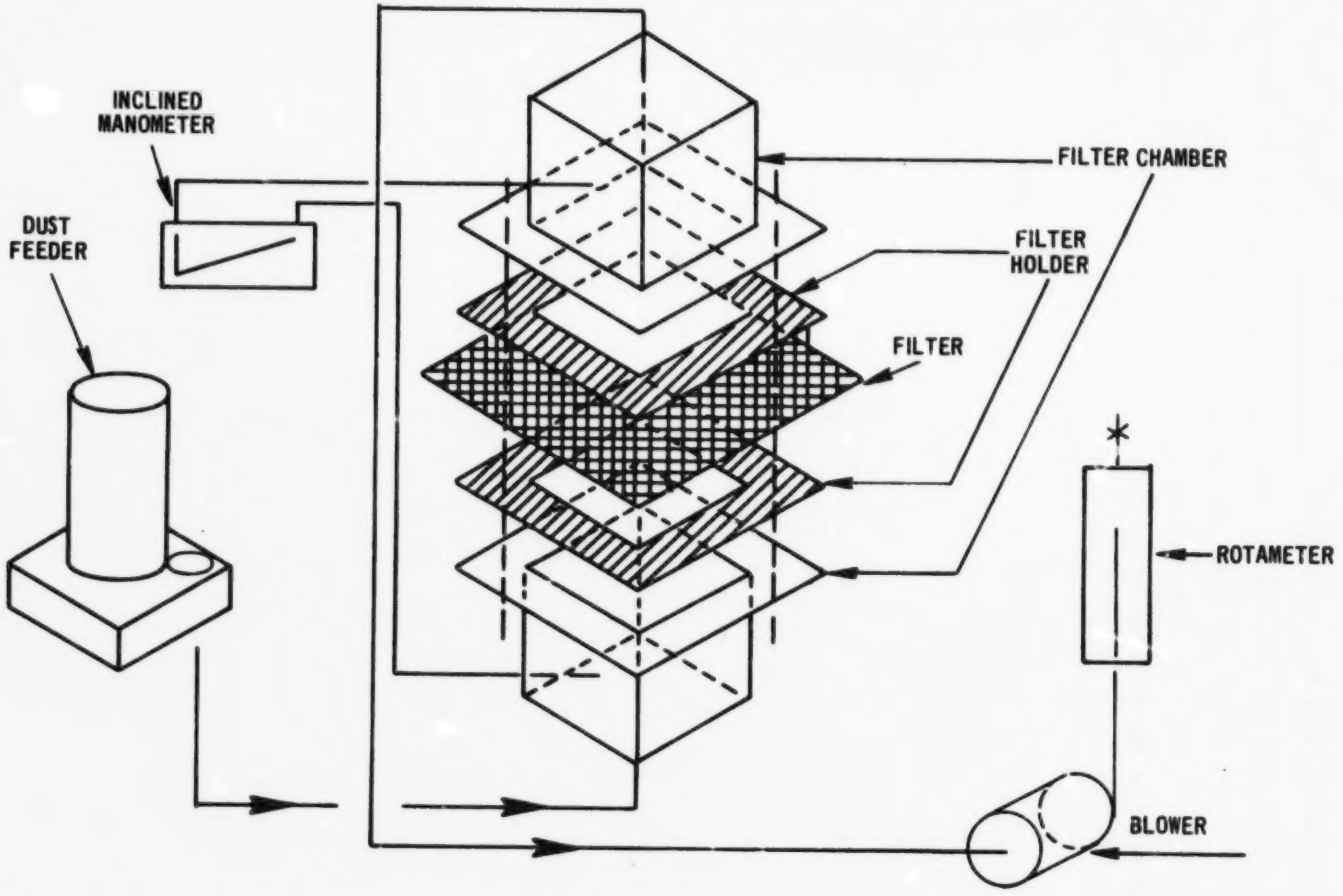

Figure 3. Bench-scale filtration apparatus.

mainly in the composition of the yarn fibers. These fabrics are listed in Appendix D with supplemental fabric characterization test data. The filter bags sewn from these fabrics were 3.58 in. in diameter and roughly 71.0 in. in overall length, with a 2-in. cuff on each end. Flow and dust feed were adjusted to maintain dust loading and filter ratio at the same values used for the previously tested 123 fabrics. The same four responses were used to describe the performance of these fabrics.

RESULTS AND DISCUSSION

SINGLE-COMPARTMENT BAGHOUSE STUDY--FREE-AREA CORRELATION WITH PRESSURE-RELATED FILTRATION RESPONSE

An attempt was made to correlate single-compartment baghouse filtration performance of statistically chosen blocks of fabrics against structural features of the fabrics such as weave, warp count, fill count, and yarn type (staple or continuous). The results of this type of correlation were poor.

An attempt was then made to correlate filtration performance of groups of fabrics against more fundamental structural features shown by the supplemental test data in Appendix E (available on request). Clean cloth Frazier permeability (CFM at 0.5 in. H_2O) was found to correlate with pressure performance (ΔP_f, S_e, K), but not with outlet concentration (C_o). A "free area", calculated for each fabric, was found to provide a better correlation with pressure performance and a weak correlation with the outlet concentration of the filter fabrics.

The free area for each fabric was calculated from yarn count and yarn width data as follows:

$$FA \text{ (free area)} = 1 - (W_c W_w + F_c F_w - W_c W_w F_c F_w) = [1 - \text{cover factor}]$$

where

subscript c = count, threads per in.

subscript w = yarn width, in.

W = warp

F = fill

The free area is simply a measure of the total pore area of the fabric, measured from a direction normal to the fabric's surface (i.e., a projected pore area). A cover factor greater than 1 for either the warp or the fill yarns alone implies a free area of 0.0.

This section of the report presents results and a discussion of filtration performance of four groups of fabrics. Each group was selected to study the effects of specific fabric structural variables on filtration performance. The four groups of fabrics and the structural variables for each group are:

Group 1 - Warp count, fill count, and yarn type (continuous filament or staple fiber).

Group 2 - Fiber (Dacron or nylon) and yarn type (continuous filament or staple fiber).

Group 3 - Fill count and napping.

Group 4 - Weave and yarn type (continuous filament or staple fiber).

Group 1 Fabrics

The first group of fabrics analyzed is listed in Table 1, along with filtration performance data and calculated free area values. The pressure-related performance data are plotted against calculated free areas in Figures 4 and 5. Figure 6, showing outlet concentration, indicates an obvious lack of a consistent relationship. This first group of fabrics consists of a balanced set with a high and a low warp and fill count for continuous-continuous, continuous-staple, and staple-staple warp-fill yarn combinations, respectively (Table 1).

The effective drag, final pressure drop, and the resultant K values are inverse functions of the free area. Very low free areas, implying very small straight-through flow paths for the fabrics tested, lead to more erratic results. Data for all fabrics except fabric 34 appear to correlate well against free area. There is some doubt of the accuracy of the yarn width measurements on fabric 34 (Frazier permeability of 113.0 CFM at 0.5 in. H_2O), because its permeability and performance are very similar to those of fabric 33 (Frazier permeability of 84.4 CFM at 0.5 in. H_2O); however, the calculated free area is quite different.

Table 1. FREE AREA AND PERFORMANCE DATA -- GROUP 1 FABRICS (DACRON)

Fabric No. (Refer to Appendix A)	Thread Count W x F (threads/in.)	Yarn Width (in.)		Calculated free area	Outlet concentration (grains/10^3ft^3)	ΔP_f (in. H_2O)	S_e $\left(\frac{\text{in. } H_2O}{\text{fpm*}}\right)$	K $\left(\frac{\text{in. } H_2O/\text{fpm*}}{\text{lb/ft}^2}\right)$
		Warp	Fill					
5[a]	64 x 54	0.01543	0.01490	0.002	88.7	3.12	0.48	9.14
8[a]	64 x 82	0.01490	0.01357	0.0	1.92	4.31	0.78	8.60
9[a]	76 x 54	0.01303	0.01436	0.002	50.3	4.23	0.69	10.97
15[a]	76 x 82	0.01323	0.01700	0.0	8.10	4.34	0.80	8.50
30[b]	64 x 54	0.01380	0.00945	0.057	175	0.70	0.11	2.06
33[b]	64 x 82	0.01350	0.00864	0.039	268	1.69	0.26	5.00
34[b]	76 x 54	0.01350	0.00972	0.0	273	1.46	0.13	7.03
41[b]	76 x 82	0.01242	0.00864	0.017	33.5	3.21	0.56	7.20
116[c]	64 x 54	0.00886	0.00890	0.249	275	0.25	0.03	1.10
$\frac{118 + 119^c}{2}$	64 x 82	0.00830	0.01051	0.074	140	0.60	0.10	1.50
73[c]	76 x 54	0.00839	0.00945	0.178	154	0.52	0.09	1.80
88[c]	76 x 82	0.00894	0.01083	0.036	106.5	1.08	0.18	3.15

[a] Continuous filament 250/50 warp and fill

[b] Continuous filament 250/50 warp -- staple 250 equivalent denier fill

[c] Staple 250 equivalent denier warp and fill

* fpm = ft/min.

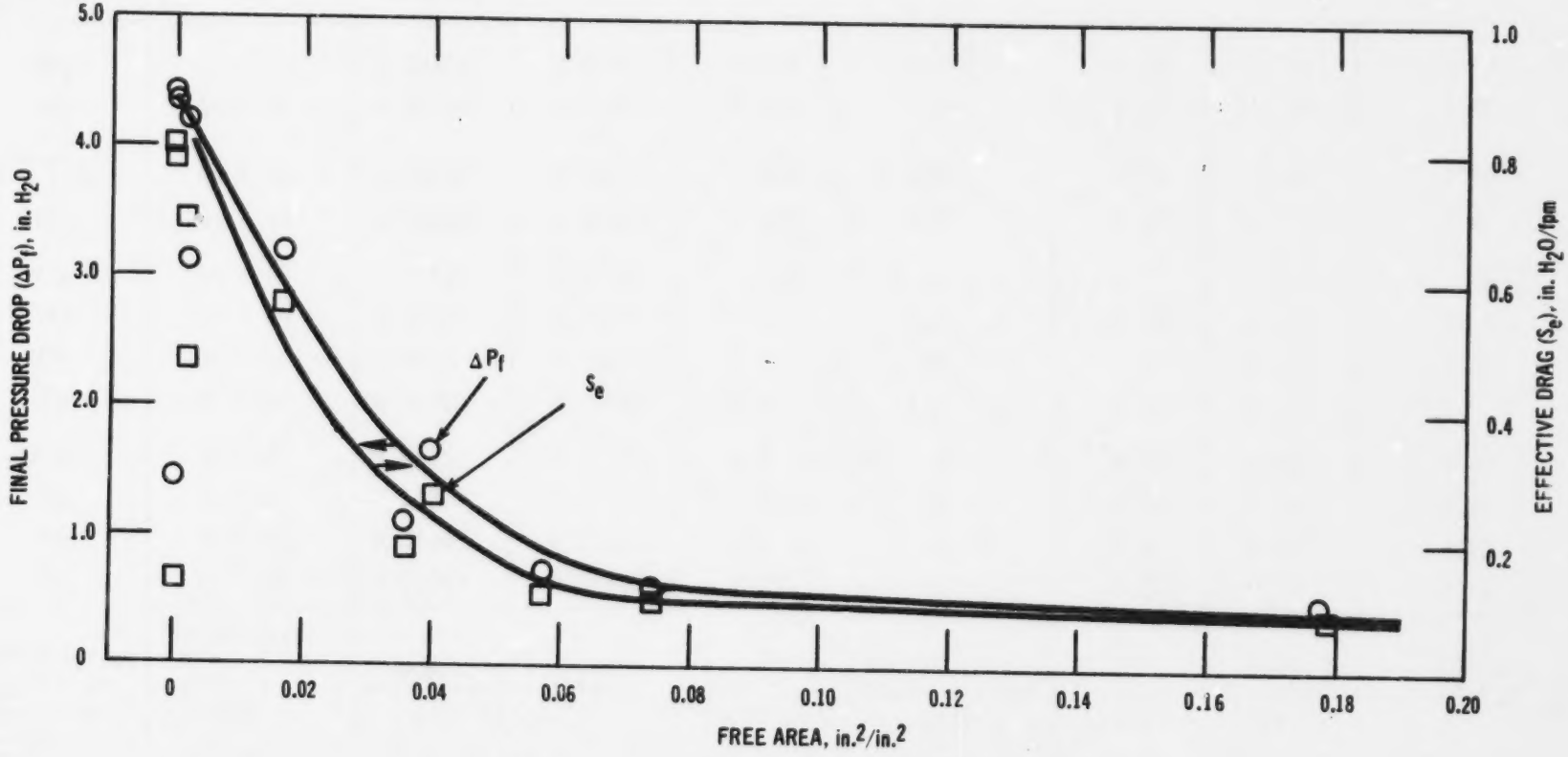

Figure 4. ΔP_f and S_e versus free area--group 1 fabrics.

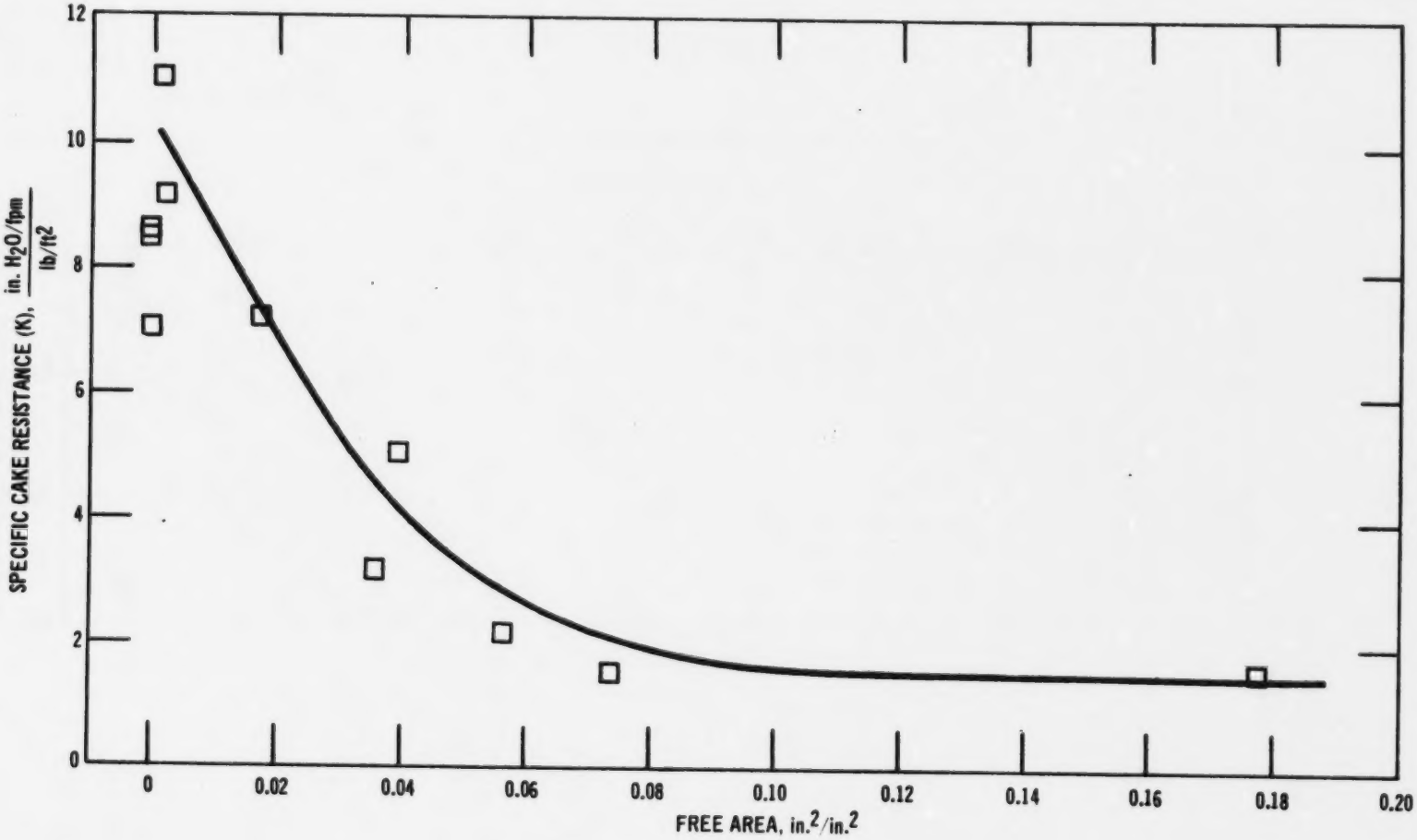

Figure 5. K versus free area--group 1 fabrics.

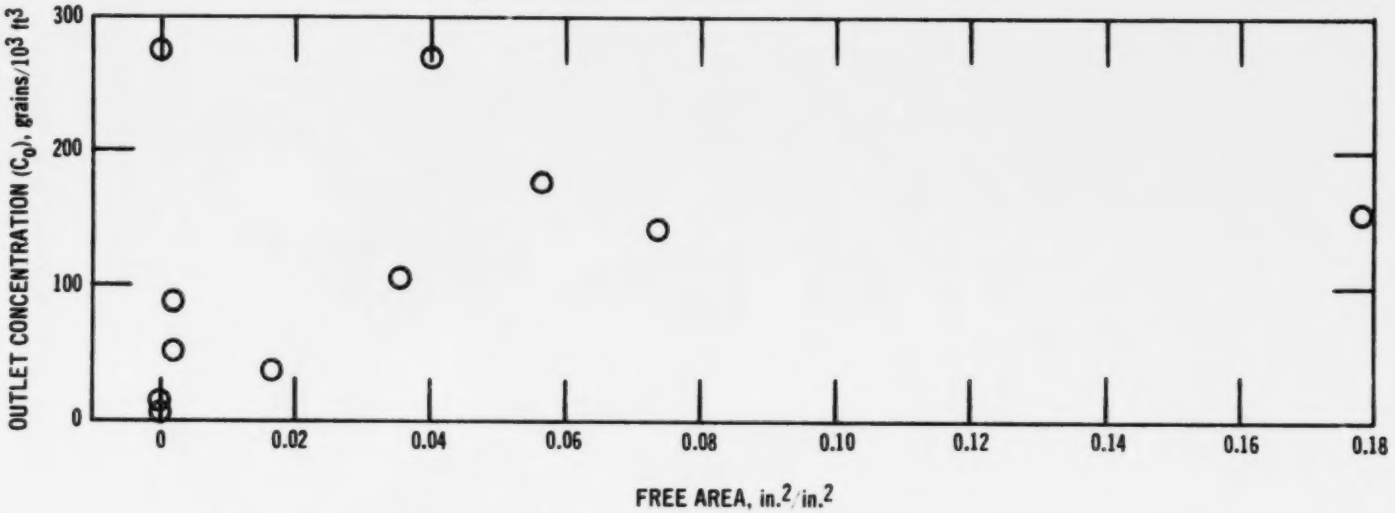

Figure 6. C_o versus free area--group 1 fabrics.

Group 2 Fabrics

A second group of fabrics was analyzed in the same manner as Group 1. The second group of fabrics was not a balanced set: it represented extreme limits in warp and fill counts and contained both Dacron and Dacron-nylon fabrics with various yarn types. The pressure-related performance data for these fabrics (Table 2) are plotted against calculated free areas in Figures 7 and 8. The outlet concentration data again showed a weak correlation and are not plotted. Outlet concentration will be discussed in greater detail following the section on microscopic analysis of the filtration process.

The effective drag, final pressure drop, and resultant K values are again shown to be inverse functions of the free area with more erratic results occurring as the free area approaches zero. Considering the range of construction variables shown by these fabrics, the correlation is fairly good. The presence of either staple or continuous filament nylon fill yarns does not appear to cause a significant shift in any of the performance responses.

Group 3 Fabrics

The third group of fabrics represented a wide range of fill counts for staple Dacron fabrics, both unnapped and napped. The performance data and supplemental test data for these fabrics are given in Table 3. Pressure-related performance data for these fabrics are plotted against calculated free areas in Figures 9 and 10.

The correlation between pressure-related performance and calculated free area for these fabrics is very good. The data points representing napped fabrics are identified. It can be seen that all of the pressure-related responses are slightly lower for the napped fabrics. Except for the fabric 91 data point, the trend is to lower the average overall pressure drop for the napped fabrics by roughly 0.12 in. H_2O without

Table 2. FREE AREA AND PERFORMANCE DATA -- GROUP 2 FABRICS

Fabric No. (Refer to Appendix A)	Thread Count W x F (threads/in.)	Yarn width (in.)		Calculated free area	Outlet concentration (grains/10^3 ft.^{3})	ΔP_f (in.H_2O)	S_e $\left(\frac{\text{in.}H_2O}{\text{fpm*}}\right)$	K $\left(\frac{\text{in.}H_2O/\text{fpm*}}{\text{lb}/\text{ft}^2}\right)$
		Warp	Fill					
Dacron Series								
1[a]	59 x 54	0.01622	0.01739	0.003	42.8	2.88	0.42	9.04
29[a]	80 x 82	0.01270	0.01220	0.0	2.30	5.40	1.12	6.09
38[b]	76 x 73	0.01269	0.00945	0.012	84.1	3.30	0.51	10.90
120[c]	59 x 54	0.00969	0.01031	0.189	261	0.17	0.01	1.12
115[c]	80 x 87	0.00862	0.00933	0.059	35.8	1.86	0.30	5.05
79[c]	76 x 68	0.00878	0.00925	0.123	185	0.67	0.10	2.01
Nylon fill Series								
45[a]	64 x 54	0.01593	0.01701	0.0	100	2.37	0.33	7.70
48[a]	64 x 82	0.01458	0.01188	0.002	30.3	4.98	0.84	12.00
50[a]	76 x 63	0.01296	0.01458	0.002	32.5	5.27	0.95	10.70
52[a]	76 x 82	0.01269	0.01134	0.002	17.6	5.01	0.96	8.00
54[b]	64 x 63	0.01269	0.01026	0.067	269	0.90	0.11	3.25
56[b]	64 x 82	0.01377	0.00972	0.025	100	1.53	0.25	3.80

[a]Continuous filament warp and fill

[b]Continuous filament warp -- staple fill

[c]Staple warp and fill

*fpm = ft/min.

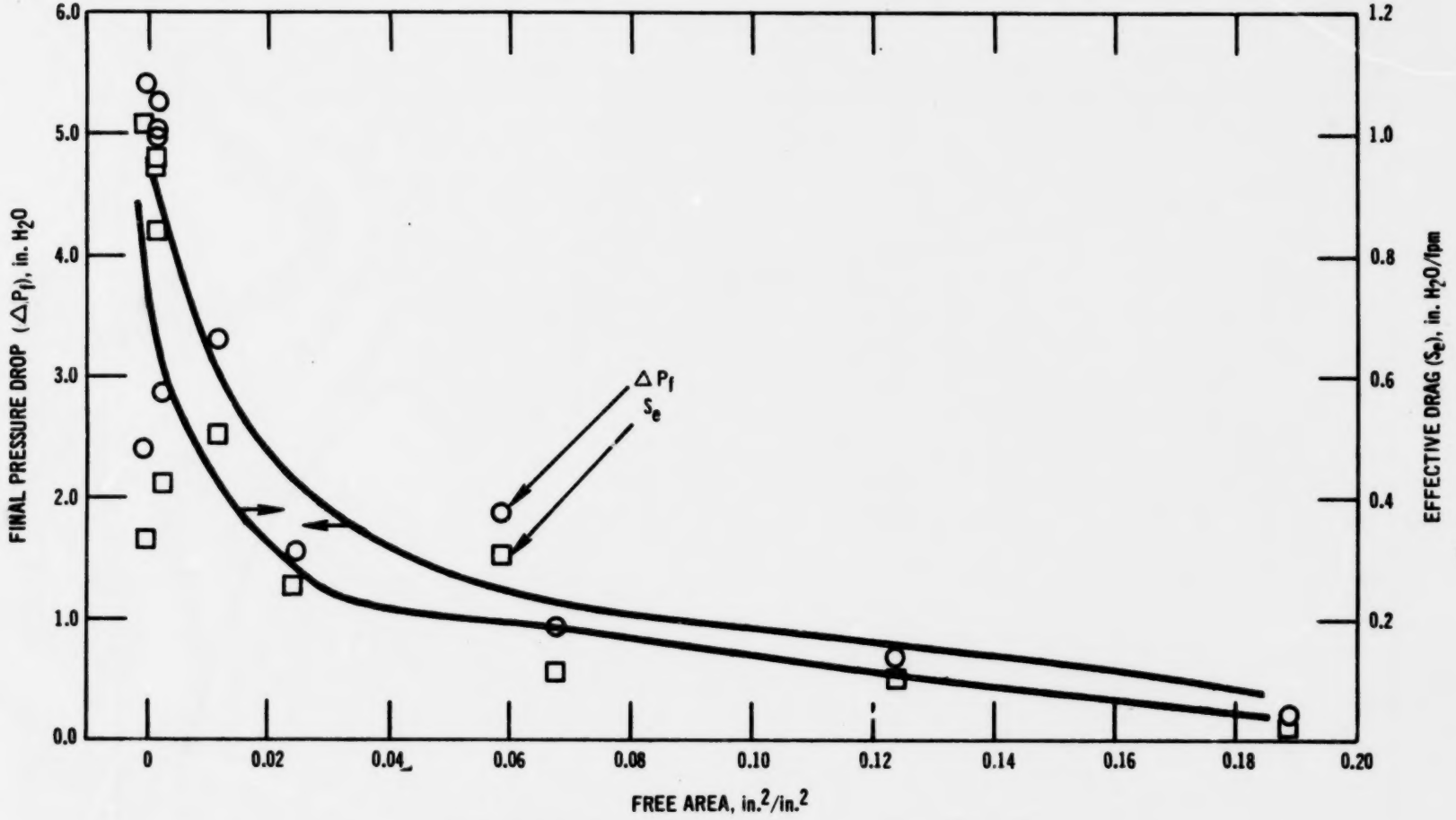

Figure 7. ΔP_f and S_e versus free area--group 2 fabrics.

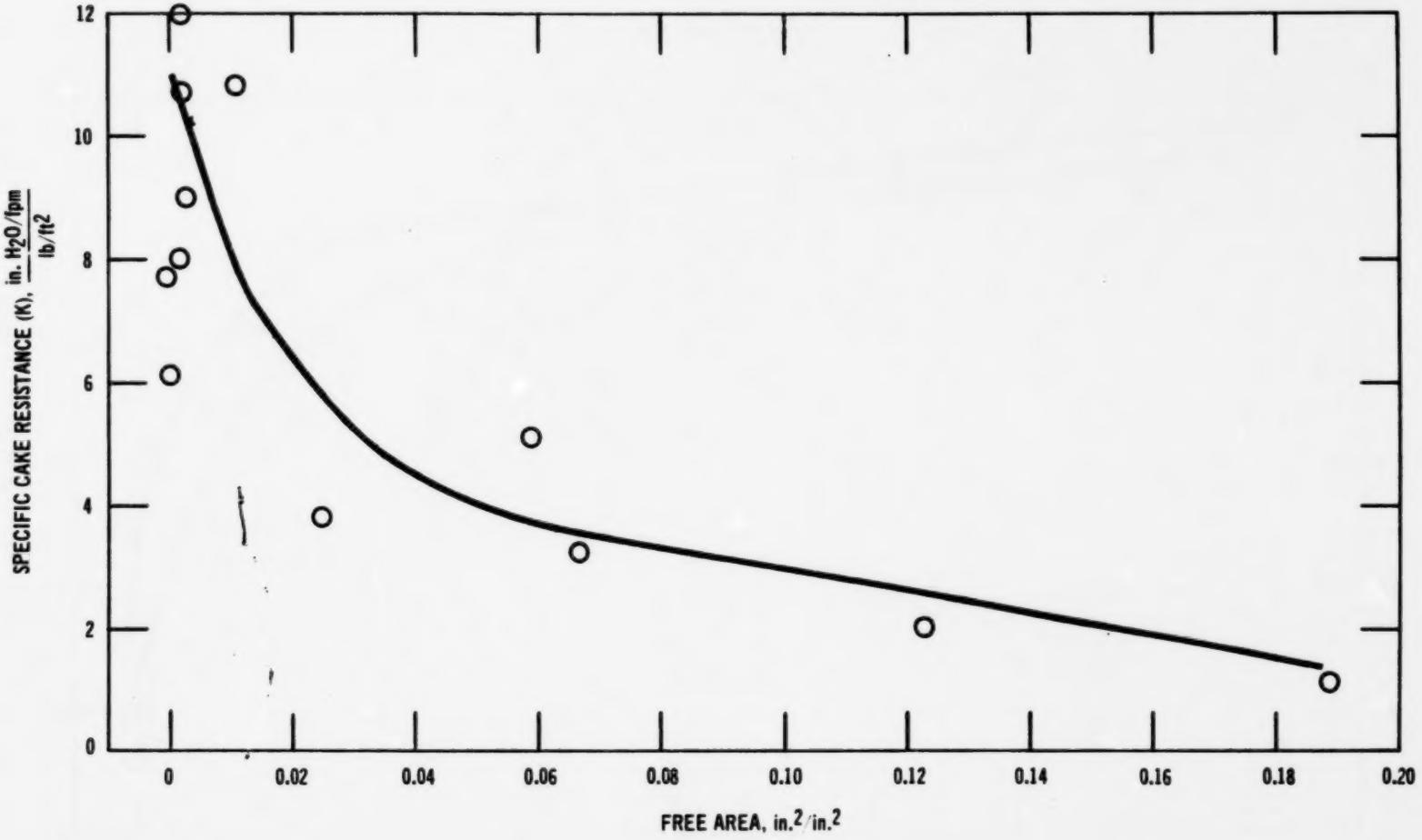

Figure 8. K versus free area--group 2 fabrics.

Table 3. FREE AREA AND PERFORMANCE DATA -- GROUP 3 FABRICS

Fabric No.[a] (Refer to Appendix A)	Thread Count W x F (threads/in.)	Yarn width (in.)		Calculated free area	Outlet concentration (grains/$10^3 ft^3$)	ΔP_f ($in.H_2O$)	S_e $\left(\frac{in.H_2O}{fpm^*}\right)$	K $\left(\frac{in.H_2O/fpm^*}{lb/ft^2}\right)$	Nap thickness (in.)
		Warp	Fill						
73	76 x 54	0.00839	0.00945	0.177	154.0	0.52	0.09	1.80	---
74[b]	76 x 54	0.00858	0.00941	0.171	78.2	0.54	0.06	2.39	0.0228
76	76 x 59	0.00854	0.00870	0.170	170.4	0.75	0.10	2.76	---
77[b]	76 x 59	0.00772	0.00937	0.185	225.6	0.57	0.06	2.42	0.0209
79	76 x 68	0.00878	0.00925	0.124	182.0	0.65	0.10	2.00	---
80[b]	76 x 68	0.00874	0.00980	0.112	61.6	0.86	0.13	2.72	0.0197
82	76 x 73	0.00894	0.00941	0.100	229.0	0.92	0.14	3.11	0.0144
83[b]	76 x 73	0.00933	0.01000	0.079	149.0	0.58	0.07	2.38	0.0232
85	76 x 78	0.00846	0.00976	0.085	242.0	1.00	0.14	3.68	---
86[b]	76 x 78	0.00909	0.01004	0.067	43.4	0.90	0.14	2.85	0.0244
88	76 x 82	0.00894	0.01083	0.036	106.5	1.08	0.18	3.15	---
89[b]	76 x 82	0.00913	0.00988	0.058	129.0	1.00	0.13	3.96	0.0244
91	76 x 87	0.00839	0.00949	0.063	131.0	1.58	0.18	6.26	---
92[b]	76 x 87	0.00898	0.01039	0.031	46.6	1.01	0.15	3.45	0.0195

[a]All fabrics staple Dacron 250 equivalent denier warp and fill

[b]Napped fabrics

* fpm = ft/min.

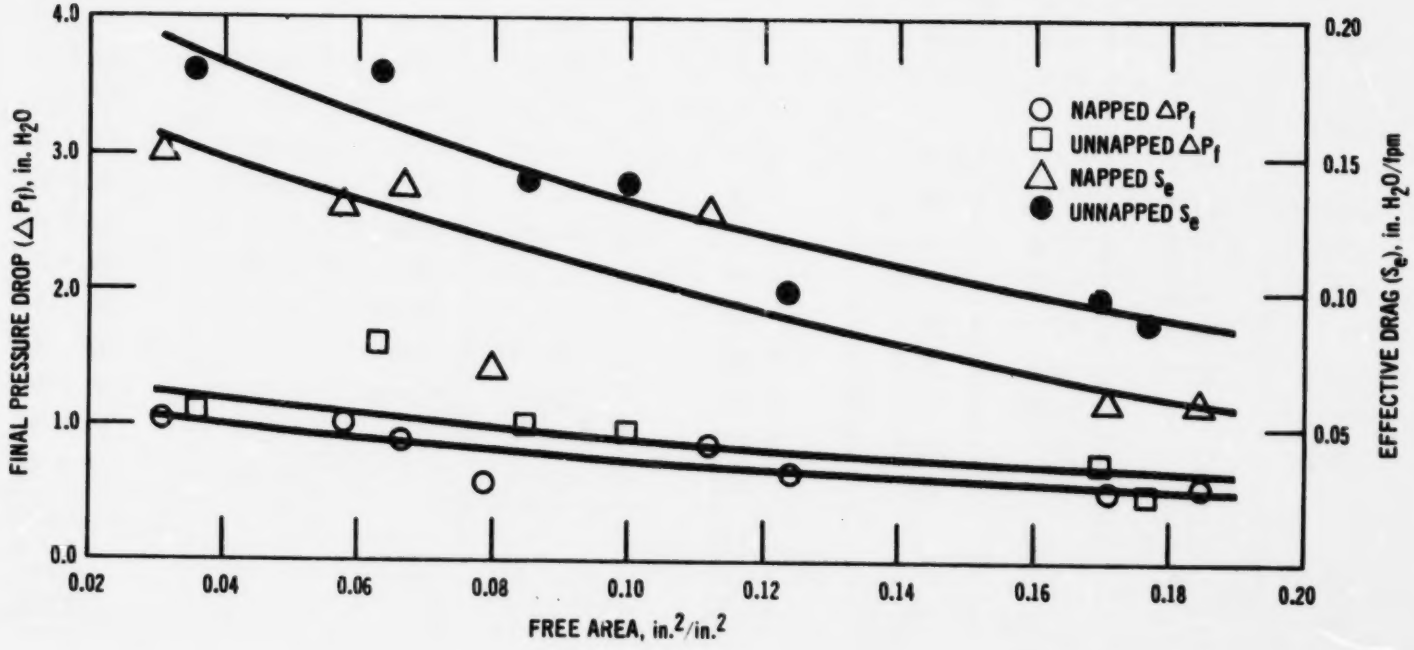

Figure 9. Δ P_f and S_e versus free area--group 3 fabrics.

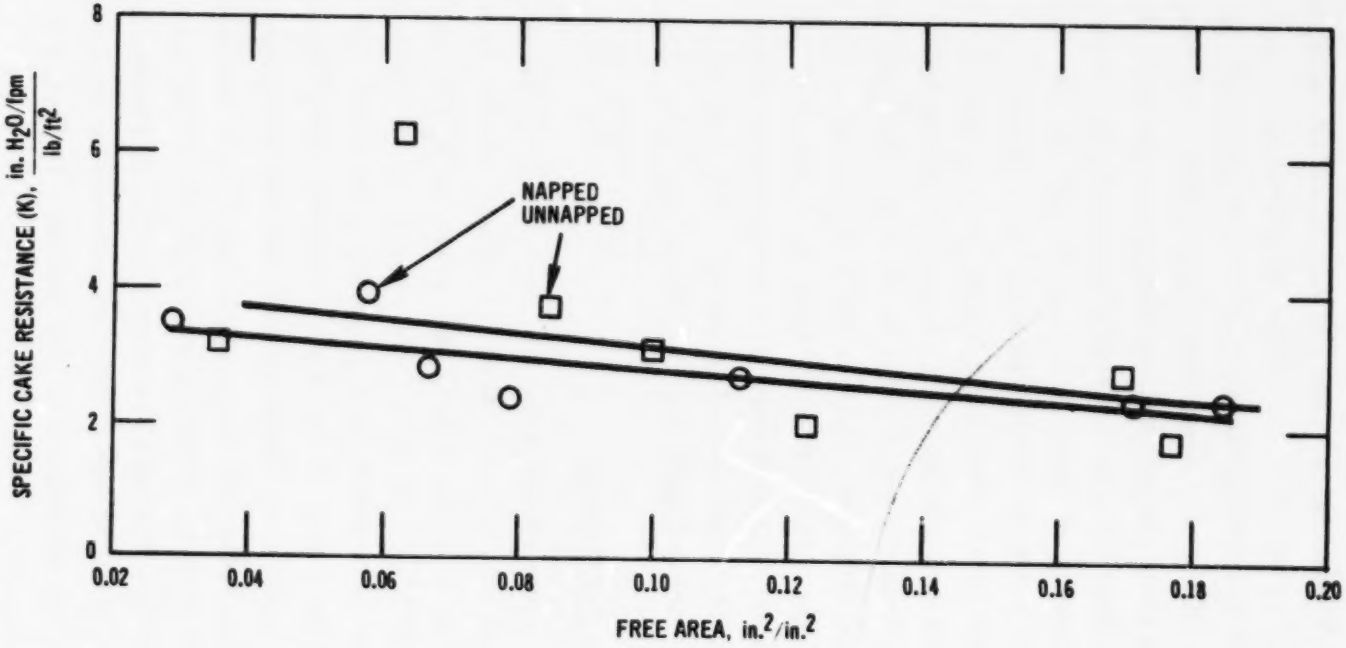

Figure 10. K versus free area--group 3 fabrics.

causing any significant differences in the rate of pressure increase as a function of time for napped versus unnapped fabrics. In other words, nap does not appear to affect the K values. A possible explanation may be that all the fabrics are fairly light (4.72 - 5.96 oz/yd^2 versus industrial fabrics generally ranging 5-14 oz/yd^2) with light napping. Actual nap thickness averages 0.01 in.; e.g., the comparison between the nap thickness for fabric 82 (unnapped) and that for fabric 83 (napped) in Table 3. A nap of 0.01 in. is really a light fuzz; it would not be considered a nap on a commercial filter fabric. These light naps result from using a yarn with a twist of 15-20 turns per in. which does not lend itself to napping. The overall effect of a light nap was to reduce average pressure drop slightly and increase efficiency significantly. These effects are probably due to the slight decrease in the number of yarn fibers as a result of the napping process and the nap or fuzz providing deposition sites for the dust which allowed fewer unobstructed large flow paths. This is discussed at greater length following Figure 15.

Group 4 Fabrics

The fourth group of fabrics represented six different weaves in both continuous filament and staple Dacron fabrics. The performance data for these fabrics are given in Table 4 and shown graphically in Figures 11 and 12. There appears to be a good correlation between free area and pressure-related performance for these fabrics. There do not appear to be any significant variations in performance solely as a result of weave, except for the much higher pressure drops produced by the plain weave fabric (not plotted). Outlet concentration data once again poorly correlate with free area and are not plotted; however, they will be discussed in following sections. These data are not adequate for a detailed examination of weave effects because the fabrics tested lie at the extremes of free area values studied.

Table 4. FREE AREA AND PERFORMANCE DATA -- GROUP 4 FABRICS[a]

Fabric No. (Refer to Appendix A)	Weave	Yarn width (in.)		Free Area	Outlet concentration (grains/10^3 ft^3)	ΔP_f (in. H_2O)	S_e $\left(\frac{\text{in. } H_2O}{\text{fpm*}}\right)$	K $\left(\frac{\text{in. } H_2O/\text{fpm*}}{lb^2/ft^2}\right)$
		Warp	Fill					
11[b]	3 x 1	0.01303	0.01410	0.001	49.1	4.77	0.83	10.60
17[b]	3 x 2	0.01404	0.01620	0.0	2.10	3.93	0.72	7.46
18[b]	2 x 2	0.01377	0.01620	0.0	3.79	4.16	0.82	6.45
19[b]	Plain	0.01296	0.01350	0.002	3.69	7.34	1.57	6.79
20[b]	Satin	0.01296	0.01647	0.0	6.89	4.37	0.83	7.51
21[b]	Crowfoot	0.01620	0.01458	0.0	2.91	4.25	0.83	6.82
94[c]	3 x 1	0.00894	0.00898	0.139	352	0.66	0.08	2.60
97[c]	3 x 2	0.00878	0.00965	0.130	141	0.79	0.13	2.73
100[c]	2 x 2	0.00807	0.00882	0.172	332	0.53	0.07	2.17
103[c]	Plain	0.00882	0.00917	0.139	187	0.60	0.09	2.18
106[c]	Satin	0.00846	0.00898	0.155	427	0.50	0.07	1.81
109[c]	Crowfoot	0.00795	0.00909	0.169	194	0.66	0.09	2.37

[a]All fabrics have 76 x 63 thread count

[b]Continuous filament 250/50 warp and fill - Dacron

[c]Staple 250 equivalent denier warp and fill - Dacron

* fpm = ft/min.

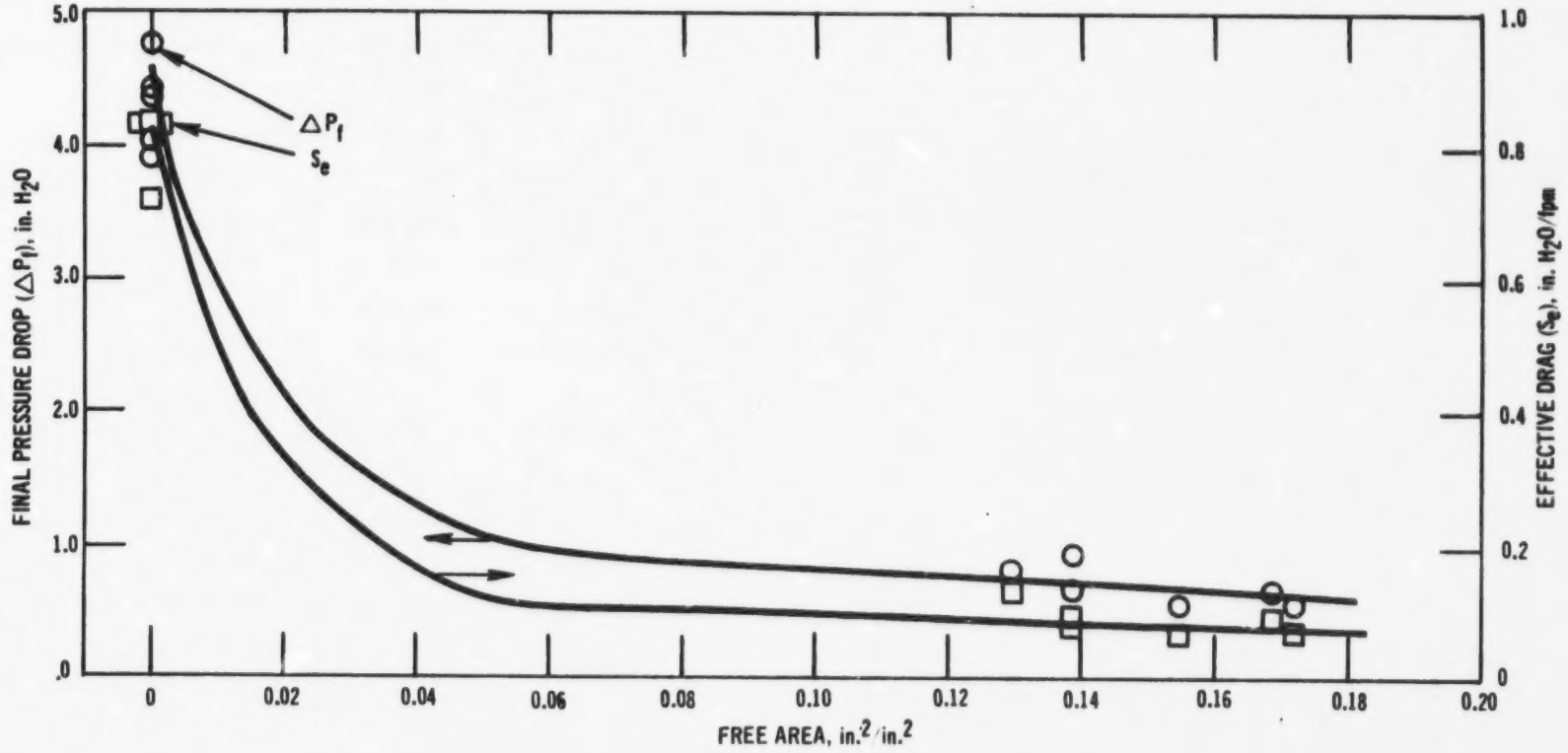

Figure 11. ΔP_f and S_e versus free area--group 4 fabrics.

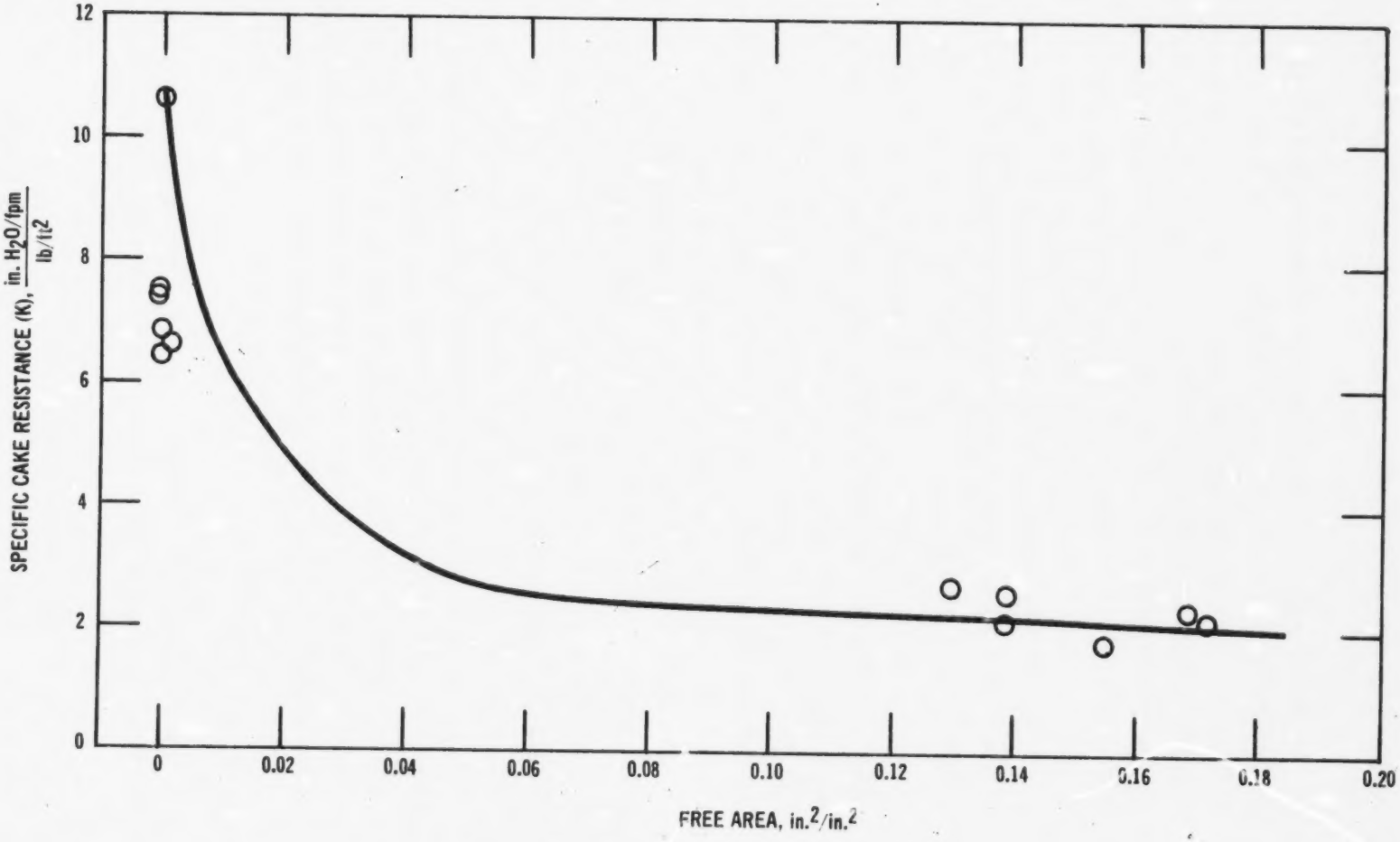

Figure 12. K versus free area--group 4 fabrics.

BENCH-SCALE FILTRATION STUDY--MICROSCOPIC ANALYSIS OF THE FILTRATION PROCESS

A bench-scale test series was conducted to further develop an understanding of fabric-structure filtration-performance relationships with emphasis on outlet concentration. Four fabrics were chosen, representing the entire range of free areas seen, for a detailed study on the bench-scale 1-ft^2 filtration apparatus. These four fabrics had shown consistent performance and uniform structure in the test studies discussed previously. A description of these fabrics, along with some of the supplemental test data, is given in Table 5. Results of the study, as well as its implications concerning the previously presented data, follow.

A series of photomicrographs was taken of four different fabrics (Table 5) from the group of 123 fabrics. These fabrics were all 3 x 1 twill weave, but differed in thread count and yarn type (continuous or staple). These differences caused a range of free areas in the fabrics. An analysis of the data has been made, partly on the basis of theoretical interstice analysis of woven fabrics done by Backer.[5] The four basic interstice types are shown in Figure 13. In the following discussion, the words "pore" and "interstice" are interchangeable.

A set of runs was made on a 1-ft^2 bench-scale filtration apparatus (Figure 3). Each clean piece of fabric was run at standard conditions (4 ft/min, 3 grains/ft^3, 30% R.H., and 70°F). No initial break-in was used because attempts to manually clean fabric samples were not reproducible. The test dust was a fine fly ash with $\bar{d}$ = 4.9μm by Coulter Counter analysis. Each fabric was removed and photomicrographed after 2, 4, 6, 8, 14, 22, and 30 minutes of filtration. A description of the photomicrographs and implications of the data follow.

Fabric 015

Initial deposition occurred almost entirely at Type II pores. Deposits continued to form at these interstices until joining together occurred. A

Table 5. FABRIC DESCRIPTION DATA FOR MICROSCOPIC ANALYSIS AND DUST/FABRIC COMBINATION STUDIES

Fabric No.	Yarn[a]		Yarn[b] count	Yarn width (in.)		Calculated free area[c]	Permeability (CFM at 0.5 in. H_2O)	Average pore dimension[d] x (μ)
	Warp	Fill		Warp	Fill			
015	Continuous, 250 denier	Continuous, 250 denier	76 x 82	0.01323	0.01701	0.001	15.0	0-10
038	Continuous, 250 denier	Staple, 210 equivalent denier	76 x 73	0.01269	0.00945	0.0109	55.0	17-35
088	Staple, 210 equivalent denier	Staple, 210 equivalent denier	76 x 82	0.00894	0.01083	0.0370	89.0	50-60
120	Staple, 210 equivalent denier	Staple, 210 equivalent denier	59 x 54	0.00969	0.01031	0.1898	432.0	~196

[a]Dacron yarn

[b]As woven

[c]Free area = (1 - cover factor)

[d]Yarn counts are not exact due to weaving procedures and handling. Average pore dimensions are calculated as a range using the yarn counts "as woven" and the actual yarn counts measured later in supplemental tests. These average pore dimensions are calculated from yarn width and yarn count data assuming square pores of dimension x.

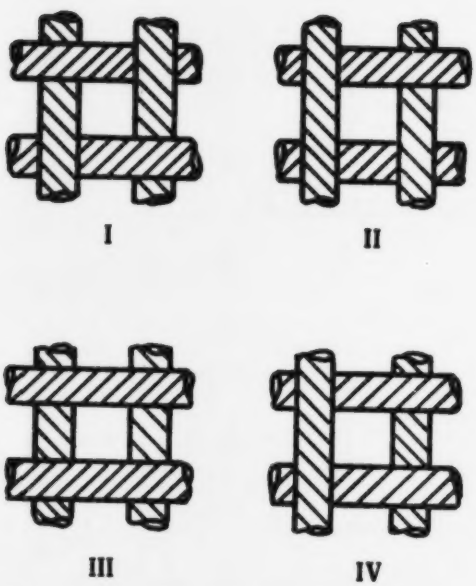

Figure 13. The four interstice types.

uniform dust cake was formed at t = 14 minutes. Initial pressure drop was high (ΔP_i = 1.27 in. H_2O), relative to the other fabrics tested in this series. Pressure increase was gradual, giving ΔP_f = 1.62 in. H_2O and K = 2.98. Very limited deposition occurred at Type III pores due to the spreading out of the continuous-filament yarns when unrestrained by an adjacent cross yarn (refer to Appendix C on weave yarn interactions). No deposition occurred at Type I pores. Weight gain was roughly 14 grams out of 24.6 grams fed, or 56.9%.

Fabric 038

Initial deposition occurred almost entirely at Type II pores. Dust continued to deposit at these pores, forming very dense deposits. The pores appeared to have a significant depth relative to the total fabric thickness. Dust deposition remained below the fabric surface until t = 8 minutes and, thus, no joining of deposits started until this point. The deposits gradually joined together, aided by some deposition on the few fibers projecting above the fabric's surface. A relatively uniform dust cake did not appear to form until t = 22 minutes. Initial pressure drop ΔP_i = 0.59 in. H_2O and a steep rise in the ΔP versus t curve gave ΔP_f = 1.06 in. H_2O and $K \tilde{=} 4.37$. Weight gain was 11.8 grams out of 22.5 grams fed, or 52.3%.

Fabric 088

Initial deposition occurred mainly at Type II and III pores, with less uniform deposits forming at Type I pores. Deposits built up gradually both in and around the pores and on fibers projecting above the surface of the fabric. A rough, fairly continuous dust cake was formed at t = 22 minutes. Pinhole leaks occurred through the fabric and dust throughout the 30-minute cycle. Initial pressure drop, ΔP_i, was 0.18 in. H_2O. Pressure increase was gradual, giving ΔP_f = 0.4 in. H_2O and K = 2.94. Yarn spacing was not uniform, causing a wide range of pore dimensions. Weight gain was 8.2 grams out of 22.47 grams fed, or 36.5%.

Fabric 120

Initial deposition occurred very slowly. Dust built up gradually, bridging over the smaller pores first. Bridging and dust buildup were significantly affected by individual fibers projecting above the fabric's surface and across individual pores to which large deposits of dust became attached. A continuous dust cake never formed due to the presence of a number of extremely large pores (~400μm) which the dust could not bridge. Pinhole leaks occurred throughout the 30-minute cycle. Deposition occurred without preference to pore type. Initial pressure drop was very low, ΔP_i = 0.03 in. H_2O. Pressure rose slowly to ΔP_f = 0.10 in. H_2O, giving K = 1.22. Weight gain was 6.3 grams out of 22.5 grams fed, or 28.0%.

During experimental runs with a standard $\bar{d}$ = 4.9μm fly ash test dust, the analysis showed that pinhole leaks occurred through fabrics 088 and 120, but not through fabrics 015 and 038. These fabrics had a range of free areas of from ~ zero to 18.9%. Table 5 shows the free area and an average pore dimension for each fabric, calculated from yarn width measurements and yarn count. Yarn counts measured in the supplemental fabric testing varied slightly from the fabric specifications as ordered. The range for pore sizes given in Table 5 indicates the difference in the calculated values using the "as ordered" count or the measured yarn count. (Note: It should also be noted that both dust size distributions and pore size distributions are polydisperse and that an average or mean value does not completely describe such size distributions.) Billings and Wilder[6] have postulated that a given dust can bridge roughly 10 particle diameters. The test dust used for the experimental work was fly ash with $\bar{d}$ = 4.9μm by Coulter Counter analysis. Fabrics 015 and 038 have typical average pore dimensions of less than 10 particle diameters for the $\bar{d}$ = 4.9μm dust. Fabrics 088 and 120, on the other hand, have typical average pore dimensions of more than 10 particle

diameters. As mentioned earlier pinhole leaks were not observed through fabrics 015 and 038, but were observed through fabrics 088 and 120. To check the hypothesis on dust bridging, another test with $\bar{d}$ = 10μm was prepared from a coarser blend of the same fly ash. This test dust was run with fabric 088 in a manner identical to the other bench-scale experimental runs. The following results were observed.

Fabric 088 ($\bar{d}$ = 10μm Test Dust)

Initial deposition occurred mainly at Type II and III pores with somewhat less heavy deposits at Type I pores. Dust built up fairly rapidly on the surface of the fabric and on projecting fibers to form a rough, fairly continuous dust cake at t = 10 minutes. Some pinhole leaks were observed throughout the 30-minute cycle. Initial pressure drop, ΔP_i, was 0.24 in. H_2O. Pressure drop increased gradually, giving ΔP_f = 0.66 in. H_2O and K = 2.88. Weight gain was 17.35 grams out of 24.45 grams fed, or 71.0%.

A comparison was made between the photomicrographs of fabric 088 using $\bar{d}$ = 4.9μm and $\bar{d}$ = 10μm test dust. Measurements were made of the minimum pinhole size over the entire 30-minute cycle by manually measuring pinhole dimension shown in photomicrographs at 100x.

Table 6 shows the smallest pinhole size measured for each dust at each time interval, as well as the average over the cycle. The average minimum pinhole dimension over the 30-minute cycle was 48μm with fly ash of $\bar{d}$ = 4.9μm, and 100μm with fly ash of $\bar{d}$ = 10μm. These measurements, although approximate, show strong support of a dust's ability to bridge roughly 10 particle diameters under the aerodynamic conditions existing in a fabric filter. All other factors being equal, the increased dust retention with the coarser dust suggests reduced bleeding through the fabric because of fewer pinhole leaks.

Table 6. MINIMUM PINHOLE SIZES DURING A FILTER CYCLE

Time (min.)	Dust size (microns)	
	4.9μm	10μm
2	40	70
4	40	110
6	50	70
8	50	50
14	60	150
22	--	120
30	--	130
Average	48	100

SINGLE-COMPARTMENT BAGHOUSE STUDY--DUST-SIZE/PORE-SIZE CORRELATION WITH FILTER EFFICIENCY

Filtration Performance of Dust/Fabric Combinations

To add further support to the proposed relationship between dust size, pore dimensions, and bleeding phenomena, additional runs were conducted using the single-compartment baghouses to study the effect of changing the dust type on the relation between pore dimensions and outlet concentration. Fabrics 015, 038, 088, and 120 (Appendix A) were tested using: fly ash dust with a mass mean particle diameter of 3.7μm; limestone dust with a mass mean particle diameter of ∿18.5μm; and amorphous silica dust with a mass mean particle diameter of ∿17.0μm. Standard test conditions were used: filter ratio of 4.0 ft/min; inlet dust concentration of 3.0 grains/ft^3; relative humidity of 30% at ∿70°F; and a 20-minute filter cycle with 24 hours of break in. Filtration performance results are shown in Table 7 for these three dusts.

Comparing the outlet concentration data for the three dusts tested with the rough pore dimensions given in Table 7 shows that none of the dusts tested produced significant outlet concentrations unless the fabric on which they were being filtered had a rough average pore dimension on the order of 10 times the mass mean particle diameter. Pressure drops and K values differed drastically between these dusts.

A comparison between the outlet concentration data in Table 7 for limestone and silica dust indicates that, once a threshold is reached where significant bleeding may occur, the magnitude of the outlet concentration may be partially dependent on the pressure drop during the filtration cycle. In addition, it should be noted that K values may vary considerably as a function of fabric while outlet concentration remains relatively constant. This indicates that pressure-related performance may be optimized while maintaining high efficiency.

Table 7. FILTRATION PERFORMANCE DATA FOR DUST/FABRIC COMBINATIONS

Dust	Performance response	Fabric No. 015	038	088	120
Fly ash, $\bar{d}$ = 3.7μm	Outlet concentration (grains/10^3ft^3)	8.0	84.0	106	261
	ΔP_f (in. H_2O)	4.34	3.33	1.09	0.18
	S_e $\left(\frac{\text{in. } H_2O}{\text{ft/min}}\right)$	0.80	0.51	0.18	0.01
	K $\left(\frac{\text{in. } H_2O/(\text{ft/min})}{\text{lb/ft}^2}\right)$	8.50	10.95	3.15	1.12
Limestone, $\bar{d}$ = 18.5μm	Outlet concentration (grains/10^3ft^3)	8.62	4.51	11.4	142
	ΔP_f (in. H_2O)	7.86	5.79	3.21	0.77
	S_e $\left(\frac{\text{in. } H_2O}{\text{ft/min}}\right)$	1.37	0.92	0.44	0.40
	K $\left(\frac{\text{in. } H_2O/(\text{ft/min})}{\text{lb/ft}^2}\right)$	15.32	13.98	11.49	4.93
Amorphous silica $\bar{d}$ = 17.0μm	Outlet concentration (grains/10^3ft^3)	2.96	2.86	1.48	272
	ΔP_f (in. H_2O)	15.74	11.33	6.45	2.56
	S_e $\left(\frac{\text{in. } H_2O}{\text{ft/min}}\right)$	2.21	1.58	0.61	0.01
	K $\left(\frac{\text{in. } H_2O/(\text{ft/min})}{\text{lb/ft}^2}\right)$	43.52	33.18	27.19	18.36
Average pore dimensions (microns)		0-10	17-35	50-60	~196

Another interesting observation concerns the pore types (Figure 13) at which dust deposition occurred. Backer[5] indicated that the four main interstice types can be used to predict clean-cloth permeability if a fabric is considered to have a close-packed warp; i.e., if adjacent warp yarns touch. The relative minimum void cross-sectional areas from the close-packed warp model indicate minimum flow through Type III pores with greater flow through Type I, II, and IV pores, respectively. The fabrics containing continuous-filament warp yarns approximate a close-packed warp model because of the high warp yarn cover factor resulting from very low yarn twist. The fabrics with continuous-filament warp yarns showed dust deposition (indicating gas flow) at the various pore types in proportion to the relative flows indicated by the close-packed warp model. The fabrics containing staple warp yarns, on the other hand, represent a cylindrical yarn model because of the lower yarn cover factors resulting from high yarn twist. The fabrics with staple warp yarns showed less uniform dust deposition (indicating gas flow) which did not correspond well to the relative flows indicated by a close-packed warp model.

Theoretical analysis, such as that done by Backer[5], provides a baseline for understanding flow through fabrics. Assumptions about fabric structure, such as the close-packed warp model, are useful if tempered with an understanding of the effects of weave and yarn type. Constraints on yarn cross-section dimensions, such as the twist on staple yarns, strongly affect structure with respect to flow and filtration. A more detailed discussion of effects of weave and weave yarn interactions is presented in Appendix C.

It was noted that the free areas and the pores of the 123 fabrics studied were much smaller for the continuous-filament fabrics, than for the staple yarn fabrics, due to the former's higher yarn cover factors. Yarn width and thickness data, along with outlet concentration data, for selected fabrics are presented in Table 8. Although the weight of fiber per unit area is roughly the same for both the staple and continuous-filament fabrics, the continuous-filament fabrics are much more efficient

Table 8. RELATIVE YARN DIMENSIONS FOR CONTINUOUS-FILAMENT VERSUS STAPLE YARNS COMPARED TO OUTLET CONCENTRATION DATA

Fabric No.	Weave	Yarn construction (Dacron)	Average yarn width (in.)	Average yarn thickness (in.)	Fabric weight (oz/yd^2)	Outlet concentration (grains/10^3 ft^3)
011	3 x 1	Continuous-filament, 250 denier	0.01356	0.00467	4.66	49.1
019	Plain		0.01296	0.00456	4.42	3.69
020	Satin		0.01296	0.00457	4.60	6.89
094	3 x 1	Staple, 210 equivalent denier	0.00894	0.00728	5.13	352.0
103	Plain		0.00882	0.00634	5.16	187.0
106	Satin		0.00846	0.00705	4.83	427.0

filters due to the more elliptical yarn cross sections which provide a higher yarn cover factor and a more uniform positive barrier to dust. This difference in yarn cross-sectional shape results from the high twist on the staple yarns relative to the very low twist on the continuous-filament yarns.

Cross-sectional dimensions of continuous-filament yarns are more subject to change from adjoining cross yarns than are those of staple yarns. This implies an interaction between yarn type and weave that influences relative flow through the various pore types (refer to Appendix C).

The previous discussion of bench-scale filtration tests reveals fabric structural features responsible for filtration performance. For the fabrics tested, flow and dust deposition are primarily at Type II pores. The free area, a measure of the average minimum pore area in a normal direction (calculated from yarn width measurements) is a good indication of the pressure-related performance. The weave interacts somewhat with the yarn to determine actual flow patterns. Pores which are open to straight-through flow are subject to bleeding as they increase in size; a critical pore size for bridging purposes occurs at roughly 10 $\bar{d}$ of the dust being filtered. Thus, the pore size distribution in a direction normal to the flow is largely responsible for outlet concentration.

Filtration Performance of Commercial Fabrics

The previous paragraph does not consider fiber properties, such as composition and surface characteristics. To check the effect of fiber composition, a group of nine commercially available fabrics was purchased and fabricated into filter bags of dimensions as stated in the equipment and procedures section. These bags were then run on the single-compartment baghouses, using the $\bar{d}$ = 4.9μm fly ash test dust and filtration conditions as specified previously. Performance data are given in Table 9 for these fabrics.

Table 9. FILTRATION PERFORMANCE DATA -- FABRIC COMPOSITION STUDY

Fabric No.	Yarn		Weave	Thread count W x F (threads/in.)	Fiber type	Outlet concentration (grains/10^3ft^3)	ΔP_f (in. H_2O)	S_e $\left(\frac{\text{in. } H_2O}{\text{fpm*}}\right)$	K $\left(\frac{\text{in. } H_2O/\text{fpm*}}{\text{lb/ft}^2}\right)$
	Warp	Fill							
1-39703	250 d. Dacron, type 55	250 d. Dacron type 55	3 x 1	78 x 65	Polyester	6.71	6.11	1.29	6.68
2-39707	250 d. Dacron, type 55	250 d. Dacron type 55	3 x 1	68 x 54	Polyester	52.0	2.35	0.36	6.55
3-39577	200 d. Dralon	200 d. Dralon	3 x 1	78 x 70	Acrylic	3.92	4.02	0.79	5.95
4-4589	Spun acrylic, 12.00/1	Spun acrylic 12.00/1	3 x 1	76 x 51	Acrylic	3.45	2.75	0.50	5.00
5-33106	210 d. poly-propylene	210 d. poly-propylene	3 x 1	67 x 53	Polypropylene (olefin)	422	2.33	0.22	9.48
6-39704	250 d. Dacron type 55	250 d. Dacron, type 55	3 x 1	67 x 58	Polyester	89.0	3.22	0.49	8.27
7-889	Spun rayon, 21.00/1	Spun rayon, 14.00/1	Satin	96 x 86	Cellulose	38.9	1.94	0.21	7.58
8-4388	Filament polyester, 250 d./1	Spun poly-ester 16.50/1	3 x 1	77 x 77	Polyester	2.92	3.82	0.76	5.74
9-4400	Spun Nomex 16.50/2	Spun Nomex 16.50/2	Plain	46 x 38	Polyamide	6.05	3.08	0.54	6.50

*fpm = ft/min

The four fabrics selected previously for a microscopic analysis of the filtration process had well defined yarn boundaries and the free areas calculated appeared to accurately describe the pore size properties of the fabrics. Yarn width measurements conducted on the nine commercial filter fabrics were inaccurate and did not appear consistent with microscopic examination of the fabrics. Poorly defined yarn boundaries and the more generally polydisperse pore size distributions of the commercial fabrics resulted in a poor comparison between calculated free areas and pore size properties of the fabrics. Filtration performance of the nine commercial filter fabrics was therefore correlated against microscopic measurements of fabric pore size properties, as well as with permeability.

A straight-through pore size distribution was generated for each fabric by measurements from photomicrographs. For each interstice, a measurement was made of the minimum cross-section dimension for each distinct flow channel. A projecting fiber, when present, was considered a flow channel boundary. Figure 14 shows the minimum cross-section measurements, A and B, for the two flow channels through the pore. Dimension B is the maximum distance which a dust must bridge to seal the pore and have cake law filtration.

The fallacy of using permeability as an indication of performance can be seen by comparing fabrics 5 and 7 in Table 10. Even though fabric 7 has a higher clean cloth permeability, an examination of photomicrographs indicates that a great number of fibers project across the pores. The projecting fibers allow dust to deposit and bridge over the pores in fabric 7, leading to cake law filtration and high efficiency. The maximum size of the flow channel, as far as dust is concerned, is greatly reduced by projecting fibers within the pore. The maximum size of the flow channel, as far as the gas is concerned, is not drastically affected by projecting fibers.

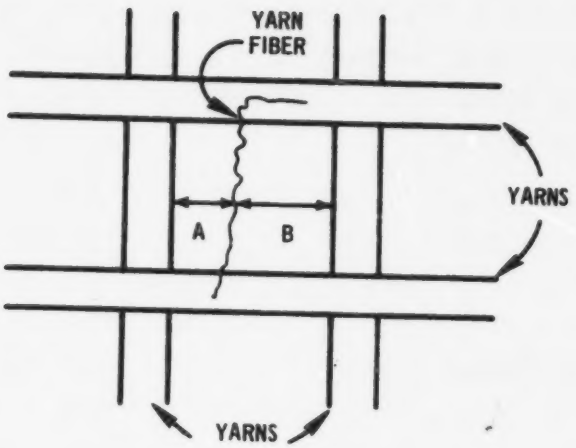

Figure 14. Pore dimensions.

Table 10. PORE SIZE DISTRIBUTIONS OF SELECTED FABRICS

(Number of pores of specified size for ~6mm^2 area.)

Fabric No.	Pore size (microns)					Outlet concentration (grains/10^3 ft^3)	Permeability (CFM at 0.5 in. H_2O)
	50μm	60μm	70μm	80μm	≥90μm		
1	2					6.0	18.5
2	1					52.0	58.8
3	---					3.9	11.5
4	---					3.4	33.0
5	3	1	3	5	5+	422.0	130.0
6	6	---	2			89.0	47.1
7	---	2				39.0	146.0
8	---					2.8	19.6
9	2					6.5	38.2

Pore size distributions were measured manually, using Polaroid photomicrographs at 100X for pores (considering projecting fibers as flow channel boundaries) visible with low substage lighting. Care was taken to avoid overexposure of photomicrographs which have led to erroneous measurements.

The pore size distributions of these nine fabrics, for the pores larger than roughly 10 times the mass mean particle diameter ($\bar{d}$ = 4.9μm), are shown in Table 10. The outlet concentration data for these fabrics show that the fabrics having significant numbers of pores larger than roughly 10 average particle diameters are by far the least efficient filters.

The significant factor, when considering outlet concentration, is a function of pore size distribution over roughly 10 times the mass mean particle size of the dust being filtered. It may be assumed that during the course of filter usage a number of the larger pores may be eliminated due to fiber or yarn rearrangement or that the dust does bridge over even very large pores but that occasional bridge collapse and bleeding do occur and are dependent on pore size.

FABRIC PARAMETERS GENERATING SIGNIFICANT DUST/FABRIC INTERACTIONS

The basic equation relating pressure drop to flow through porous beds (Equation 1) indicates that non-linear ΔP response with respect to time at constant dust and gas flow rate could be the result of changes in α. The filtration taking place could still physically be cake law filtration but the dust substrate may have changing properties. At times, the existence of cake law filtration is questioned because non-linearities are observed in ΔP vs t curves. Two examples are discussed here and an explanation is offered.

Figure 15 shows the general form of ΔP vs t curves for two different fabrics showing non-linear behavior.

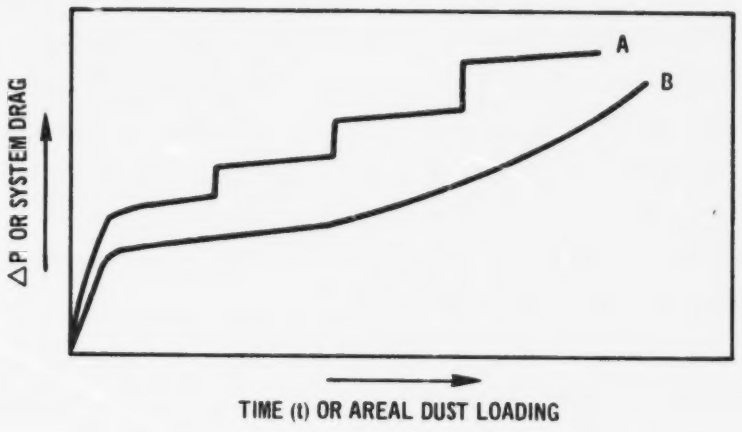

Figure 15. Non-linear ΔP versus t response.

Curve A is for fabric No. 038, a fairly light Dacron fabric with deep pores. Microscopic examination showed that heavy deposits built up in certain pores and that dust deposition took place mainly at these pores for a significant portion of the filtration cycle. The dust gradually formed a cake and a linear ΔP vs t response resulted. A dust layer built up and pressure increased until a sudden discontinuity was noted. This is known as cake collapse but is seen to occur during the normal process of filtration. Cake collapse can be precipitated by pressure increases caused by either increased gas velocity or by the continued deposition of dust. Each successive linear portion of the ΔP vs t response has a gradually lower K value, whereas the effective overall K value increases with time because of the discontinuities in the pressure increase.

Curve B is for a napped Dacron fabric where dust deposition is intimately tied to the projecting nap fibers. The non-linear ΔP vs t curve implies that the dust is being filtered by depth filtration (i.e., in the nap) and that α, the packing density, is increasing as more dust is deposited. It is expected that once the dust layer builds up above the nap-dust layer, the deposition would result in a linear ΔP vs t curve and a constant α for dust-on-dust at constant velocity (barring cake collapse under pressure).

Figure 16 illustrates a possible physical relationship between fabric structure and dust filtration. For a fabric of simple pores, a two-dimensional structure is representative.

Given 5% free area and assuming little or no intrayarn flow (this is confirmed by little deposition on yarns), it can be seen that the velocity through the pores is roughly 20 times the average face velocity. It would be unlikely to expect the same α for deposition at 4 ft/min as at 80 or 100 ft/min. Once the dust builds up above the fabric surface, filtration takes place either on previously deposited dust (region 2) or

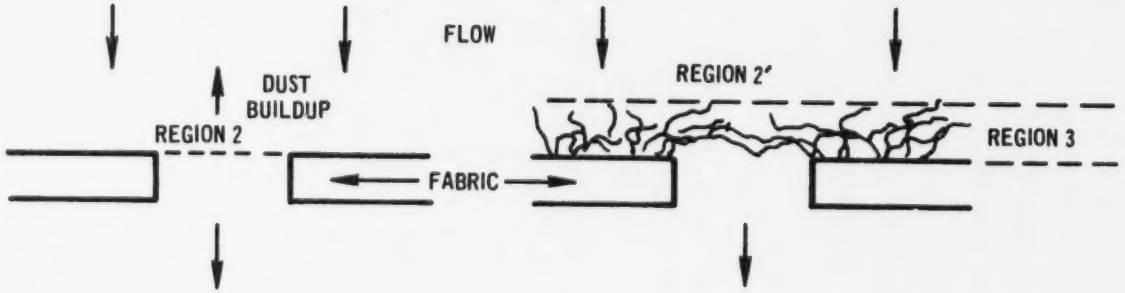

Figure 16. Schematic representation of dust/fabric interactions.

on a dust fiber matrix (region 3). If a dust fiber matrix exists, the dust eventually builds up to dust-on-dust filtration (region 2). It can be seen that there may be significant interactions between the dust and the filtering media. The dust fabric interactions are further complicated by the non-uniform flow patterns resulting from a woven fabric's heterogeneous physical structure. Since a number of physical interactions indicate probable changes in α, linear ΔP vs t responses should not necessarily be expected. Fabric structure can interact considerably with a dust to lead to unexpected pressure-related performance (Figure 16). This implies strongly that K values are not just a function of particulate structure. Care must be taken in fabric selection to guard against unexpected filtration response with respect to pressure.

An understanding of fabric structural features and their relationship to filtration performance is useful in filter design, selection, and application. Bench-scale filtration tests and simple microscopic examination of filters can be easily applied by potential makers or users of fabric filter systems to determine boundary conditions for fabric selection for the specific dust/gas system of interest. Standard Frazier permeability gives a fair indication of pressure-related filtration performance for a general fabric. Microscopic examination must be used to relate dust and fabric parameters both to ensure efficient filtration and to guard against unexpected interactions.

REFERENCES

1. Spaite, P. W. and G. W. Walsh. Effect of Fabric Structure on Filter Performance. Ind. Hygiene J.: 357-365, July-August 1963.

2. Borgwardt, R. H. and J. F. Durham. Factors Affecting the Performance of Fabric Filters. EPA. (Paper 29c, presented at 60th Annual Meeting AIChE, New York, November 29, 1967.)

3. Stephan, D. G., G. W. Walsh, and R. A. Herrick. Concepts in Fabric Air Filtration. Ind. Hygiene J. 21:1-14, February 1960.

4. Durham, J. F. and R. E. Harrington. Influence of Relative Humidity on Filtration Resistance and Efficiency of Fabric Dust Filters. Filtration and Separation: 389-392, July-August 1971.

5. Backer, S. The Relationship Between Structural Geometry of a Textile Fabric and Its Physical Properties -- Part IV, Interstice Geometry and Air Permeability. Text. Resj, October 1951.

6. Billings, C. E. and J. Wilder. Handbook of Fabric Filter Technology. NAPCA Report CPA22-69-38 (NTIS No. PB200-648), Research Triangle Park, N. C., December 1970.

NOMENCLATURE

A	filter area, ft^2
A_p	particle surface area, ft^2
C_k	coefficient in Kozeny equation, ft/min^2
C_o	outlet concentration, grains/$10^3 ft^3$ or grains/ft^3
$\bar{d}$	mass mean particle diameter, microns (μm)
E	efficiency
FA	free area
g_c	conversion factor, ft lb mass/min^2 lb force
g_l	local acceleration of gravity, ft/min^2
J	conversion factor, in. H_2O/(lb force/ft^2)
K	specific cake resistance, (in. H_2O/ft/min)/(lb/ft^2)
L	cake thickness, ft.
ΔP	pressure drop across filter, in. H_2O
ΔP_i	initial pressure drop across filter, in. H_2O
ΔP_f	final pressure drop across filter, in. H_2O
Q	air flow rate, ft^3/min
R	dust feed rate, grains/min
S_e	effective drag, in. H_2O/ft/min
u_f	fluid velocity, ft/min
V_p	particle volume, ft^3
$\bar{w}$	areal dust loading, lb/ft^2
α	cake porosity = $\frac{\text{void volume}}{\text{bulk volume}}$
u	fluid viscosity, lb mass/ft min

Preceding page blank

UNITS OF MEASURE - CONVERSIONS

Environmental Protection Agency policy is to express all measurements in Agency documents in metric units. When implementing this practice will result in undue costs or lack of clarity, conversion factors are provided for the non-metric units used in a report. Generally, this report uses British units of measure. For conversion to the metric system, use the following conversions:

To convert from	To	Multiply by
^{o}F	^{o}C	$\frac{5}{9}$ (^{o}F-32)
ft	meters	0.304
ft^2	$meters^2$	0.0929
ft^3	$meters^3$	0.0283
ft/min (fpm)	centimeters/sec	0.508
ft^3/min	$centimeters^3$/sec	471.9
in.	centimeters	2.54
$in.^2$	$centimeters^2$	6.45
oz	grams	28.34
oz/yd^2	$grams/meter^2$	33.89
grains	grams	0.0647
$grains/ft^3$	$grams/meter^3$	2.288
lb. force	dynes	4.44×10^5
lb. mass	kilograms	0.453
lb/ft^2	$grams/centimeter^2$	0.488
in. H_2O/ft/min	cm. H_2O/cm/sec	5.00
$\frac{\text{in. } H_2O/\text{ft/min}}{lb/ft^2}$	$\frac{\text{cm } H_2O/\text{cm/sec}}{gm/cm^2}$	10.24

Preceding page blank

APPENDIX A

DESCRIPTION OF 123 TEST FABRICS

I. Multifilament-Dacron Series (with 250/50 Dacron Warp Fiber)[a]

Fabric No.	Description of fill fiber	Weave	Thread count
1	250/50 Dacron[a]	3 x 1 Twill	59 x 54
2	"	"	59 x 64
3	"	"	59 x 73
4	"	"	59 x 82
5	"	"	64 x 54
6	"	"	64 x 63
7	"	"	64 x 73
8	"	"	64 x 82
9	"	"	76 x 54
10	"	"	76 x 59
11	"	"	76 x 63
12	"	"	76 x 68
13	"	"	76 x 73
14	"	"	76 x 78
15	"	"	76 x 82
16	"	"	76 x 87
17	"	3 x 2 Twill	76 x 63
18	"	2 x 2 Twill	76 x 63
19	"	Plain	76 x 63
20	"	Satin	76 x 63
21	"	Crowfoot	76 x 63
22	"	3 x 1 Twill	70 x 54
23	"	"	70 x 63
24	"	"	70 x 73
25	"	"	70 x 82
26	"	"	80 x 54
27	"	"	80 x 63
28	"	"	80 x 73
29	"	"	80 x 82
30	Staple Dacron (250 equivalent denier)	"	64 x 54
31	"	"	64 x 63
32	"	"	64 x 73
33	"	"	64 x 82
34	"	"	76 x 54
35,36[b],37[c]	"	"	76 x 63[d]
38,39[b],40[c]	"	"	76 x 73[d]
41	"	"	76 x 82
42,43[b],44[c]	"	"	76 x 87[d]

Preceding page blank

APPENDIX A (Continued)

Fabric No.	Description of fill fiber	Weave	Thread count
45	210/34 Nylon[a]	3 x 1 Twill	64 x 54
46	"	"	64 x 63
47	"	"	64 x 73
48	"	"	64 x 82
49	"	"	76 x 54
50	"	"	76 x 63
51	"	"	76 x 73
52	"	"	76 x 82
53	Staple Nylon (210 equivalent denier)	"	64 x 54
54	"	"	64 x 63
55	"	"	64 x 73
56	"	"	64 x 82
57	"	"	76 x 54
58,59[b],60[c]	"	"	76 x 63[d]
61	"	"	76 x 73
62	"	Plain	76 x 63
63	"	3 x 1 Twill	76 x 82
64	300/50 Rayon	"	76 x 63
65,66[b],67[c]	Staple Rayon (300 equivalent denier)	"	76 x 63[d]
68	"	Plain	76 x 63
69	250/50 Dacron.[a] Fine metal wire every 10th yarn in warp.	3 x 1 Twill	76 x 54
70	"	"	76 x 63
71	"	"	76 x 73
72	"	"	76 x 82

APPENDIX A (Continued)

II. Staple-Dacron Series (250 Equivalent Denier, Dacron Fiber)

Fabric No.			Weave Pattern	Count
73	74[b]	75[c]	3 x 1 Twill	76 x 54[d]
76	77[b]	78[c]	"	76 x 59[d]
79	80[b]	81[c]	"	76 x 68[d]
82	83[b]	84[c]	"	76 x 73[d]
85	86[b]	87[c]	"	76 x 78[d]
88	89[b]	90[c]	"	76 x 82[d]
91	92[b]	93[c]	"	76 x 87[d]
94	95[b]	96[c]	"	76 x 63[d]
97	98[b]	99[c]	3 x 2 Twill	76 x 63[d]
100	101[b]	102[c]	2 x 2 Twill	76 x 63[d]
103	104[b]	105[c]	Plain	76 x 63[d]
106	107[b]	108[c]	Satin	76 x 63[d]
109	110[b]	111[c]	Crowfoot	76 x 63[d]
112			3 x 1 Twill	80 x 54
113			"	80 x 63
114			"	80 x 73
115			"	80 x 87
116			"	64 x 54
117			"	64 x 63
118			"	64 x 73
119			"	64 x 87
120			"	59 x 54
121			"	59 x 63
122			"	59 x 73
123			"	59 x 87

[a]Continuous-filament

[b]Light nap

[c]Heavy nap

[d]Triple order--enough fabric to produce 30 bags: 10 regular, 10 light nap, and 10 heavy nap

APPENDIX B

STANDARD FABRIC AND YARN CHARACTERIZATION TESTS

I. Fabric Analysis

1. Type of Weave Pattern - 3x1 twill, plain, satin, etc./ASTM D 1910-64
2. Thread Count (warp and fill) - threads/in./ASTM D 1910-64
3. Fabric Weight - oz/yd^2 fabric/ASTM D 1910-64
4. Crimp (warp and fill) - percent/ASTM D 1910-64
5. Fabric Thickness - in./ASTM D 1777-64
6. Air Permeability - cfm air/ft^2 of fabric at 0.50 in. H_2O pressure drop/ASTM D 737.69
7. Bulk Density - grams fabric/cm^3 fabric
8. Type of Yarn (warp and fill) - continuous filament, staple, or combination
9. Abrasion Resistance of Textile Fabrics-ASTM D 1175-64T (tested warp and fill)
   a. Flexing and Abrasion Method - number and average number of cycles required to rupture a specimen, tension and pressure used, and condition of specimens.
   b. Flexing and Abrasion Method - average percentage loss of breaking strength obtained after abrasion for one or more specified number of cycles, tension and pressure used, and condition of specimens.
   c. Oscillatory Cylinder Method - percentage loss in breaking strength.
10. Stiffness of Fabrics (Cantilever Test) - flexural rigidity of the warp and the filling separately and an overall average/ASTM D 1388-64
11. Tear Resistance of Woven Fabrics by Falling-Pendulum (Elmendorf) Apparatus - individual values and average tearing force in grams for each direction of tear, capacity of tester, puckering, number of tests rejected/ASTM D 1424-63

Preceding page blank

12. Breaking Load and Elongation of Textile Fabrics (Grab Test) - average breaking load, etc./ASTM D 1682-64

13. Tearing Strength of Woven Fabrics by the Tongue (Single Rip) Method (Constant-Rate-of-Traverse Tensile Testing Machines) - average tearing strength etc./ASTM D 2262-64T

II. Yarn Analysis

14. Yarn Twist - amount and direction, turns/in./ASTM 1244-69T and (where applicable) ASTM D 1422 and D 1423 (fabrics)

15. Yarn Number - cotton count, worsted count, tex, and denier/ASTM 1244-69T

16. Number of Filaments per Yarn (continuous filament only) - number/yarn

17. Filament Diameter - in.(measured from logitudinal sections at 500x magnification)

18. Diameter of Staple Fiber - in./for cotton/ASTM D 1444-63

19. Yarn Width and Thickness - in. Width -- microscopic measurement with occular filar micrometer at 12x, average of 10 measurements. Thickness - microscopic measurements from embedded sample sections at 500x.

20. Bulk Density of Yarn - grams fiber/cm yarn (calculated from linear density, yarn width, and thickness)

21. Fiber Density - grams fiber/cm^3 fiber (yarns) (calculated from vibrascopic and filament diameter measurements)

22. Thickness of Nap - in. (difference between Shirley Thickness gauge measurements at 0.01 and 1.0 psi)

23. Weight of Nap - grams nap/cm^2 cloth area (difference between cloth weights with and without nap)

24. Bulk Density of Nap - grams nap/cm^3 nap (could not be determined)

APPENDIX C

EFFECT OF WEAVE ON FILTRATION PERFORMANCE

Filtration tests were made on the bench-scale filtration apparatus (Figure 3) with each of three selected fabrics using fly ash test dust. The three fabrics had different weaves and, thus, different pore type distributions (Figure 13).

Table C1. PORE TYPE EFFECTS ON FABRIC BEHAVIOR

Fabric No.	Weave	Pore types, %				ΔP_f (in. H_2O)	ΔP_i (in. H_2O)	K, in. H_2O/fpm / lb/ft^2
		I	II	III	IV			
015	3 x 1	25	50	25	--	1.62	1.27	2.76
019	Plain	100	--	--	--	4.75	4.1	4.30
020	Satin	--	80	20	--	2.45	1.75	4.18

A description of the photomicrographs for each fabric will be made and a number of inferences will be drawn.

FABRIC 015

Deposition occurs almost entirely at Type II pores. Deposits pile up at these points and join together to form a fairly uniform dust cake at t = 14 minutes. Initial pressure drop was low (ΔP_i = 1.27 in. H_2O) and pressure increase was gradual giving ΔP_f = 1.62 in. H_2O and K = 2.76. Very limited deposition was observed at Type III pores due to the spreading out of the continuous-filament yarns when unrestrained by an adjacent cross yarn.

Preceding page blank

FABRIC 019

Plain weave fabric is composed entirely of Type I pores. Deposition occurred uniformly at all Type I pores. Initial pressure drop was high (ΔP_i = 4.1 in. H_2O) due to both the nature of the pores and tightness of the weave. Uniform deposition led to joining of the individual deposits and formation of a relatively continuous dust cake at t = 8 minutes. Pressure increase was gradual, giving ΔP_f = 4.75 in. H_2O and K = 4.30.

FABRIC 020

This fabric was a four-harness satin; i.e. yarns go over four and under one as compared to the 3 x 1 twill where a yarn goes over three and under one. The weave was not a twill and the pore type distribution was thus 80% Type II and 20% Type III (refer to Figure 13). Cross sections between cross yarns were very broad (roughly 400 versus 300 μm for the plain weave). Deposition was fairly uniform along the floats with a slight decrease at the Type III pores. Initial pressure drop was low (ΔP_i = 1.75 in. H_2O) with a final pressure drop (ΔP_f) of 2.45 in. H_2O and K = 4.18. A fairly uniform dust cake was formed at t = 8 minutes.

DISCUSSION

The K values for these fabrics were not significantly different, implying that construction effects due to weave probably are not important when considering dust cake characteristics and cake properties. In previous photomicrographs, a change in K values was noted mainly due to yarn type and pore depth.

The previous photomicrographs of fabrics with a 3 x 1 twill weave had shown deposition occurring almost entirely at Type II pores. The satin weave fabric had a greater fraction of Type II pores and it was expected that its filtration behavior would reflect this. Actually, the continuous-filament yarns spread out considerably between cross yarns and reduced effective pore area (refer to Table 8). The effect

of a more elliptical cross section with the continuous-filament yarns is shown in the clean cloth Frazier permeabilities (Table C2) for these similar fabrics.

Table C2. CONTINUOUS-FILAMENT FABRICS--PORE TYPE EFFECTS

Fabric No.	Frazier permeability	Yarn count (threads/in.)	Weave
011	35.6	76 x 63	3 x 1
019	2.17	76 x 63	Plain
020	10.8	76 x 63	Satin

Theoretical interstice analysis done by Backer[5] identifies two theoretical conceptual models of the different pore types (Figure 13). If the yarns are considered to be cylindrical, the relative minimum cross-sectional areas for the different pore types indicate increasing flow through Type I, II, IV, and III pores, respectively. If a close-packed warp model is assumed, increasing flow would be expected through Type III, I, II, and IV pores, respectively. Microscopic examination of fabrics 011, 019, and 020 show their structure to be somewhat similar to that of the close-packed warp model; fabric 020 deviates from the model because of weave/yarn interactions (Table 8); i.e., the continuous-filament yarn cross sections vary considerably as a function of position along the yarn. The permeabilities shown in Table C2 for these fabrics do not reflect behavior predicted by either of the conceptual models. Microscopic examination of fabrics 094, 103, and 109 shows their structure to be quite similar to that of the pore models, assuming cylindrical yarns. The yarns are reasonably cylindrical (Table 8) because of the high yarn twist ($\sim$ 15 turns per in.), and the fabric permeabilities reflect the relative values indicated by the conceptual model assuming cylindrical yarns (Table C3).

Table C3. STAPLE YARN FABRICS -- PORE TYPE EFFECTS

Fabric No.	Yarn count (threads/in.)	Weave	Permeability (CFM at 0.5 in. H_2O)
094	76 x 63	3 x 1	201
103	76 x 63	Plain	98.4
106	76 x 63	Satin	301

A significant effect of weave and pore type is indicated by the time needed to establish a relatively uniform dust cake. The 3 x 1 twill fabric (Fabric 015) showed deposition almost exclusively at Type II pores. Type II pores constitute only 50% of the total number of pores through fabric 015. Fabric 019 (plain weave) showed deposition at all pores because of its having 100% Type I pores. Fabric 020 (satin weave) showed deposition mainly at Type II pores (80% of its pores). The time needed for the deposits at the individual pores to join together and form a continuous cake is reduced when more deposition sites are available. This is shown by the approximate time needed to form a continuous cake on the three fabrics.

Table C4. MINUTES OF FILTRATION TO FORM CONTINUOUS DUST CAKE

Fabric No.	Time to form cake (min.)
015	14
019	8
020	8

APPENDIX D

YARN AND FABRIC ANALYSIS

I. FABRIC ANALYSIS--TEST RESULTS

Fabric style	Test 1[a] weight (oz/yd^2)	Test 2[a] yarn crimp (%)		Test 3[b] Thickness (in.)	Test 4[c] permeability of air ($ft^3/min/ft^2$)
		Warp	Fill		
1-39703	5.19	1.73	4.86	0.0114	18.5
2-39707	4.48	0.61	6.15	0.0114	58.8
3-39577	3.73	0.96	8.21	0.0114	11.5
4-4589	7.59	3.08	11.26	0.0205	33.0
5-33106	3.89	3.75	4.82	0.0118	130.0
6-39704	4.37	1.13	6.67	0.0114	47.1
7-884	6.63	4.59	3.69	0.0185	146.0
8-4388	6.70	1.87	10.18	0.0165	19.6
9-4400	7.41	5.95	9.16	0.0197	38.2

[a]ASTM D 1910-64

[b]ASTM D 1777-64

[c]ASTM D 737-69

APPENDIX D (Continued). YARN AND FABRIC ANALYSIS

II. YARN ANALYSIS--TEST RESULTS (DENIER, BULK AND FIBER DENSITY)

Fabric style	Test 9[a] denier		Test 11 bulk density (gm fiber/cm^3 yarn)		Test 12 fiber density (gm fiber/cm^3 fiber)	
	Warp	Fill	Warp	Fill	Warp	Fill
1-39703	276	299	0.729	0.847	1.43	1.38
2-39707	269	294	0.729	0.847	1.43	1.38
3-39577	193	209	0.713	0.848	1.40	1.39
4-4589	408	472	0.819	0.851	----	----
5-33106	251	245	0.585	0.641	0.96	0.95
6-39704	269	294	0.756	0.876	1.32	1.37
7-884	284	362	0.745	1.330	----	----
8-4388	276	369	0.706	1.180	1.35	----
9-4400	651	646	0.894	0.725	----	----

[a]ASTM D 1244-69T

APPENDIX D (Continued). YARN AND FABRIC ANALYSIS

III. YARN ANALYSIS--TEST RESULTS (TWIST, WIDTH, AND THICKNESS)

Fabric style	Test 8[a] yarn twist (tpi-Z)		Test 10			
			Warp		Filling	
	Warp	Fill	Width (in.)	Thickness (in.)	Width (in.)	Thickness (in.)
1-39703	3.8	4.2	0.0145	0.0052	0.0131	0.0056
2-39707	3.8	4.3	0.0169	0.0048	0.0125	0.0061
3-39577	3.7	4.2	0.0155	0.0038	0.0123	0.0044
4-4589	12.3	14.4	0.0124	0.0088	0.0143	0.0085
5-33106	7.3	7.6	0.0143	0.0046	0.0133	0.0063
6-39704	3.8	4.5	0.0170	0.0046	0.0125	0.0059
7-884	12.5	14.0	0.0116	0.0072	0.0089	0.0067
8-4388	4.6	18.6	0.0121	0.0071	0.0118	0.0058
9-4400	7.7 10.9[b]	8.2 10.7[b]	0.0186	0.0087	0.0176	0.0111

[a]ASTM D 1244-69T, D 1422, and D 1423

[b]2-ply S-twist